JOINT TRANSPORTATION
RESEARCH PROGRAM
INDIANA DEPARTMENT OF TRANSPORTATION
AND PURDUE UNIVERSITY

Determining Optimal Traffic Opening Time Through Concrete Strength Monitoring: Wireless Sensing

Zhihao Kong, Na Lu

SPR-4513 • Report Number: FHWA/IN/JTRP-2023/05 • DOI: 10.5703/1288284317613

RECOMMENDED CITATION

Kong, Z., & Lu, N. (2023). *Determining optimal traffic opening time through concrete strength monitoring: Wireless sensing* (Joint Transportation Research Program Publication No. FHWA/IN/JTRP-2023/05). West Lafayette, IN: Purdue University. https://doi.org/10.5703/1288284317613

AUTHORS

Zhihao Kong
Graduate Research Assistant
Lyles School of Civil Engineering
Purdue University

Na Lu, PhD
Associate Dean of Faculty, Acting Head, and Reilly Professor
Lyles School of Civil Engineering
Purdue University
luna@purdue.edu
Corresponding Author

JOINT TRANSPORTATION RESEARCH PROGRAM

The Joint Transportation Research Program serves as a vehicle for INDOT collaboration with higher education institutions and industry in Indiana to facilitate innovation that results in continuous improvement in the planning, design, construction, operation, management and economic efficiency of the Indiana transportation infrastructure. https://engineering.purdue.edu/JTRP/index_html

Published reports of the Joint Transportation Research Program are available at http://docs.lib.purdue.edu/jtrp/.

NOTICE

TECHNICAL REPORT DOCUMENTATION PAGE

1. Report No. FHWA/IN/JTRP-2023/05	**2. Government Accession No.**	**3. Recipient's Catalog No.**
4. Title and Subtitle Determining Optimal Traffic Opening Time Through Concrete Strength Monitoring: Wireless Sensing		**5. Report Date** February 2023 **6. Performing Organization Code**
7. Author(s) Zhihao Kong and Na Lu		**8. Performing Organization Report No.** FHWA/IN/JTRP-2023/05
9. Performing Organization Name and Address Joint Transportation Research Program 1284 Civil Engineering Building Purdue University West Lafayette, IN 47907-1284		**10. Work Unit No.** **11. Contract or Grant No.** SPR-4513
12. Sponsoring Agency Name and Address Indiana Department of Transportation (SPR) State Office Building 100 North Senate Avenue Indianapolis, IN 46204		**13. Type of Report and Period Covered** Final Report **14. Sponsoring Agency Code**

15. Supplementary Notes

Prepared in cooperation with the Indiana Department of Transportation

16. Abstract

Construction and concrete production are time-sensitive and fast-paced; as such, it is crucial to monitor the in-place strength development of concrete structures in real-time. Existing concrete strength testing methods, such as the traditional hydraulic compression method specified by ASTM C 39 and the maturity method specified by ASTM C 1074, are labor-intensive, time consuming, and difficult to implement in the field. INDOT's previous research (SPR-4210) on the electromechanical impedance (EMI) technique has established its feasibility for monitoring in-situ concrete strength to determine the optimal traffic opening time. However, limitations of the data acquisition and communication systems have significantly hindered the technology's adoption for practical applications. Furthermore, the packaging of piezoelectric sensor needs to be improved to enable robust performance and better signal quality.

In this project, a wireless concrete sensor with a data transmission system was developed. It was comprised of an innovated EMI sensor and miniaturized datalogger with both wireless transmission and USB module. A cloud-based platform for data storage and computation was established, which provides the real time data visualization access to general users and data access to machine learning and data mining developers. Furthermore, field implementations were performed to prove the functionality of the innovated EMI sensor and wireless sensing system for real-time and in-place concrete strength monitoring. This project will benefit the DOTs in areas like construction, operation, and maintenance scheduling and asset management by delivering applicable concrete strength monitoring solutions.

17. Key Words concrete, sensor, piezoelectric, electromechanical impedance, EMI, open traffic, sensing traffic opening, strength, sensing, non-destructive testing, NDT, wireless, database, Internet of Things, IoT	**18. Distribution Statement** No restrictions. This document is available through the National Technical Information Service, Springfield, VA 22161.

19. Security Classif. (of this report) Unclassified	**20. Security Classif. (of this page)** Unclassified	**21. No. of Pages** 44 pages	**22. Price**

Form DOT F 1700.7 (8-72) Reproduction of completed page authorized

EXECUTIVE SUMMARY

Introduction

Construction and concrete production procedures are time-sensitive and fast-paced. These factors make it crucial to monitor the strength of concrete in real-time. Existing concrete strength testing methods, such as the traditional hydraulic compression method specified by ASTM C 39 and the maturity method specified by ASTM C 1074, can neither meet the fast pace of construction projects nor reflect the realistic mechanical property of the in-place concrete. For example, the curing condition of samples for ASTM C 39 testing can be distinct from the realistic curing condition of in-place concrete, which will cause a discrepancy between the cylinder strength and in-place concrete strength. The maturity method collects in-place temperature data; however, the correlation between the temperature profile and the strength profile varies with concrete mixtures, which makes the maturity calibration process time-consuming and expensive. Previous research (SPR-4210) on the Electromechanical Impedance (EMI) technique has approved the feasibility of monitoring in-situ concrete strength to determine the optimal traffic opening time. Specifically, a polymer-coated piezoelectric square disk was used as the EMI sensor and the Root Mean Square Deviation (RMSD) was used as the metric to interpret the compressive strength of concrete. However, the limitations of the data acquisition and communication systems have significantly hindered the adoption of the technology for practical application. Furthermore, the packaging of the piezoelectric sensor needs improvement to enable robust performance and better signal quality.

In this project, a wireless concrete EMI data transmission system was developed and was comprised of the innovated EMI sensor and a miniaturized impedance analyzer datalogger with both wireless transmission and a USB module. A cloud-based platform for data storage and computation was established, which provided real-time data visualization access to general users and data research access to machine learning and data mining developers. Machine learning models were developed to automatically process the EMI spectrum data in lieu of using hand-crafted signal features. Furthermore, field implementations have been performed to prove the functionality of the innovated EMI sensor and wireless sensing system for real-time and in-place concrete strength monitoring. This project will benefit the DOTs in maintenance scheduling and asset management by delivering practical concrete strength monitoring solutions.

Findings

In this project, the research team made systematic and comprehensive efforts to realize a practical concrete strength monitoring solution that can be deployed in real concrete projects. Both lab and field experiments were implemented to investigate the performance of the developed sensing system. The proposed sensor was tested in concrete made of Ordinary Portland Cement (OPC) and Portland Limestone Cement (PLC) containing various water-cement ratios and cured under various conditions. The data transmission performance of the datalogger was evaluated through field testing. The accuracy of the machine learning model was studied by comparing it with traditional compressive testing results. The major findings of this project are as follows.

1. Findings related to the wireless concrete EMI data transmission system.

    - Wireless technologies, such as Bluetooth, Low Power Long Range (LoRa), Wi-Fi and Long-Term Evolution (LTE, a standard for wireless broadband communication for mobile devices and data terminals) were explored. The research suggests that LoRa has challenges transferring the EMI spectrum because of the limits on unit packet size for data transmission, and Wi-Fi has challenges with the accessibility of routers on the construction site. Bluetooth and LTE were superior alternatives because of their data transmission capability and network accessibility. In this project, Bluetooth was used for wirelessly transmitting EMI spectra data packets in short-range distance from sensors to a centralized on-site hub. LTE was used for long-range distance transmission directly from sensors to the carrier towers.

2. Findings related to the on-chip EMI data acquisition and data processing system.

    - The traditional commercially available impedance analyzer weighs about 35 pounds and costs about $30,000. In this project, a customized EMI datalogger the size of a cellphone was developed at an affordable cost (about $200) based on the impedance analyzer chip AD5933. Configurations and combinations of oscillators, analog-to-digital converters, digital-to-analog converters, operational amplifiers, and circuit components were explored to build the datalogger for the concrete sensor. The datalogger was powered by rechargeable batteries that can sustain the device on site for about 1 month. The experiment results show that EMI data from the customized datalogger matched with the commercial impedance analyzer under the specific data acquisition conditions that are needed for concrete.

3. Findings related to the cloud platform for data storage and computation.

    - A cloud computing platform with the capacity for data storage, computation, and AI-assisted data processing was built to make better use of collected data and process abundant information. Such a platform includes the database, the website frontend, and computing backend. The database stored EMI spectrum data received from dataloggers. The website provided the general users with a visualized concrete data display, such as the strength and temperature profiles. The computing backend processed the data from a database using machine learning models and sent the results to the website for display.

4. Findings related to the innovated EMI sensor.

    - In this project, the EMI sensor was improved in both structure and material. A larger piezoelectric element was used to achieve higher signal to noise ratio. A cup-shape wave guide made of rubber was used to generate more prominent signal features, such as the resonant peaks. Finite Element (FE) simulation showed that the proposed sensor can measure the resonant frequencies of concrete, and such frequencies shift according to the change of concrete dynamic elastic modulus.

The simulation results also showed that a wave-filed distribution pattern surrounding the sensor can be used to describe the sensing region.

5. Findings related to the concrete experiment.

   - Concrete experiments were conducted for OPC and PLC concrete, along with various water cement ratios (0.42, 0.45, 0.50, 0.55) and various specimen shapes (beam, slab). Field testing was implemented at paving projects at Bass Road, Fort Wayne, Indianapolis Airport Runway, and I-35E Highway in Hillsboro, Texas. Results indicate that the regression model has R square of 0.86 for lab testing and R square of 0.64 for field testing. The research team is working on advanced data processing methods, such as machine learning, to improve the accuracy of strength interpretation from EMI spectrums.

Implementation

The wireless sensing system, including the EMI sensor and the datalogger are found to be applicable for real-time and as a replacement for concrete strength monitoring. The sensor is disposable whereas the datalogger is reusable, so this product is affordable compared with the cost of traditional compressive cylinder testing. The datalogger provides users with convenient features, such as the wireless data transmission, which enables remote monitoring, and the USB cord data pulling, which serves as a backup solution when a network is not available in distant areas.

The deliverables of this project have the potential to be an alternative to traditional strength testing. They could also be leveraged to reduce material overdesigning and carbon emission and improve pavement maintenance efficiency.

CONTENTS

LIST OF TABLES

LIST OF FIGURES

1. INTRODUCTION

1.1 Research Background

Concrete structures are often exposed to substantial loading even at their early age, which may cause premature failure or significant reduction in their life span. Therefore, it is critical to develop an in-situ NDT method that can determine the mechanical properties of concrete in real-time. In particular, the static elastic modulus (the stress-strain relationship of the concrete in its elastic stage) makes it one of most important mechanical properties in concrete structures.

The traditional method to determine the static elastic modulus of concrete is the uniaxial compressive strength test of cylinder samples as described in ASTM C469. The elastic modulus measured in the uniaxial direction is so called Young's modulus. Besides the ASTM C469, ASTM C215, ASTM E1876 and literature (Kolluru et al., 2000) provide resonance-based NDT methods to calculate the dynamic modulus of concrete specimens using natural frequencies. These NDT methods are convenient to implement compared to traditional compressive tests due to the ease of experimental setup and operation; however, they require operators to accurately locate the positions of the driving point, the support point, and the receiver point (as shown in Figure 1.1), which makes it not feasible for in-situ field implementations.

In contrast, the EMI technique has been approved to be a reliable in-situ method to determine cementitious material properties including the compressive strength and Young's modulus in lieu of conducting traditional hydraulic compression test (Lu et al., 2018; Shin et al., 2008; Su et al., 2019). In principle the EMI technique uses piezoelectric materials such as Lead Zirconate Titantate (PZT) as transducers to detect the mechanical properties of host structures, due to its ability to directly convert mechanical vibration to AC current and vice versa (Fan et al., 2018; Feng et al., 2019; Hou et al., 2019; Kong et al., 2013; Wang et al., 2018; Zhang et al., 2019). PZT sensors vibrate and interact with the host structure which generate electrical signals of admittance and impedance that can reflect the mechanical properties of a host structure correspondingly.

The EMI technique can measure dynamic modulus with one single sensor. It is convenient for in-situ testing of concrete structures because the testing procedure only involves bonding the sensor on the specimen surface or embedding it in a specimen then connecting it to impedance analyzer. Other stress wave-based techniques such as Ultrasonic Pulse Velocity (UPV) (Bogas et al., 2013) and Impact Resonance (IR) require at least a pair of transmitter and receiver in the setup. Therefore, the EMI technique realized significant saving in time, labor, and cost.

However, existing EMI methods for determining the dynamic modulus and strength of concrete have limitations in the following aspects.

1. The existing EMI sensors are usually made of a piezoelectric element with coating layers. The radiated acoustic wave field is not regulated, so the EMI signal is dominated by the interfacial properties of the sensor. The material being measured is basically just the cement paste around the sensor. This makes the evaluation on the dynamic modulus of concrete too localized to represent the volumetric material property.
2. The physical mechanisms that explain the correlation between the EMI spectrum and dynamic modulus are limited. Literature (Bhalla & Soh, 2004a, 2004b; Liang et al., 1994; Wang et al., 2014) developed mathematical models where the contribution of a host structure to the electrical spectrum of a PZT sensor was expressed as the effective structural mechanical impedance. The effective mechanical impedance is an abstractive metric of the host structure that simplifies the contribution of the host structure as the interfacial interaction with the PZT sensor. However, existing studies did not discuss the contribution of volumetric material properties to that of effective mechanical impedance, which is a potentially useful knowledge to understand broader area of material properties surrounding the PZT sensor rather than just the interfacial area.
3. The EMI spectra vary between sensors even if they are attached to identical host structures. This can be attributed to the sensor variability and the boundary condition variability of sensors. As such, the repeatability of the EMI method is difficult to be ensured. Literature (Narayanan, et al., 2017; Wang et al., 2014) suggest extracting a free PZT spectrum from the experimental results to treat the variation of sensors during the signal processing but this approach is based on 1D assumption of the vibration equation of the PZT which has limited applications. To address

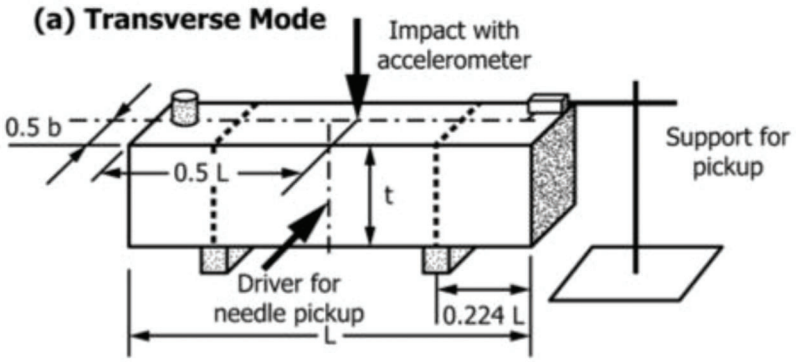

Figure 1.1 ASTM C215 testing.

the above-mentioned issues, a method of quantitative measurement of dynamic elastic modulus of a concrete using the EMI spectrum of a novel piezoelectric sensor is introduced in this study. This method is based on the viability of the measurement of resonant frequency of the concrete using such sensor. It has the clear physical meaning (vibration mode) rather than just correlation between the inputs and target values. Besides the dynamic elastic modulus, the proposed method is also used to determine the concrete strength, which is influenced by more variables than the dynamic elastic modulus, such as the sample size, the concrete aggregate content, the moisture content, etc.

1.2 Objectives

The goal of this study aims to investigate the in-place NDT testing method using a novel piezoelectric acoustical sensor along with innovated EMI resonance method on monitoring the concrete dynamic modulus and strength. Unlike conventional inefficient destructive testing, the study will monitor the variations in the EMI spectrum of the sensor embedded in concrete to determine the mechanical properties (dynamic modulus and strength) of concrete. Ultimately, this study will develop a solution that can be practically used by contractors and make the construction process easier. The main objective and contribution of this study can be summarized as follows.

1. Proof-of-concept of using the sensor spectrum to measure the host structure resonance.
   Few literatures make use of the peaks in EMI spectrum other than the peaks caused by the resonance of piezoelectric element. This study will explore the method to make use of such peaks to perform structural health monitoring. The idea will be firstly validated using concrete cylinders (3 inches by 6 inches). These cylinders are small so a piezoelectric sensor can excite the global vibration and measure the cylinder's resonance. The resonant frequencies of the EMI spectrum of the sensor will be compared with the resonant frequencies of the concrete cylinders measure by traditional impact resonance method specified in ASTM C215.
2. Improvement on the sensor packaging.
   The piezoelectric sensor is packaged with more robust materials and structures. Numerical simulation is used to determine the details of the sensor like the geometry design and material selection. The simulation is also used to visualize the measurable range of this sensor. The sensor will be prototyped then fabricated. The fabrication work involves adjusting materials and designs based on realistic resources and simulation results.
3. Experimental study on the performance of the fabricated sensor.
   The sensor is designed to excite the resonant mode of the concrete inside the waveguide the sensor. The measured resonant frequency is used as the metric to determine the elasticity of host structure (concrete). The correlation between such metric and the target value will be studied through experiment. The reliability and variability of fabricated sensor also will also be examined through experiment. Concrete with various material mixtures, sample sizes, shapes and curing conditions will be made to evaluate the performance of the proposed sensor.

1.3 Organization of the Report

This report consists of six chapters. This first chapter introduces the background and objective of this research. The second chapter reviews existing concrete strength estimation methods, including the destructive and nondestructive testing methods. The third chapter explains the working mechanism of the proposed sensor and the numerical simulation work. The fourth chapter presents the laboratory mortar and concrete testing. The fifth chapter introduced the field implementation of the proposed sensing system. The final chapter summarizes the current works and recommendations for practical usage.

2. LITERATURE REVIEW

2.1 Traditional Testing Methods for Strength of Concrete

Compressive strength testing is a widely used method for measuring the strength of concrete. This method involves applying a compressive load to a concrete specimen until it fails (Figure 2.1), and then measuring the maximum compressive load. This method is relatively simple and commonly used by the industry as the standard to determine concrete strength. However, this method can be subject to errors due to the difficulty of achieving uniform loading and the potential for specimen size effects. Literature (del Viso et al., 2008) studied the size and shape effect on the compressive strength of concrete and reported that specimens with higher slenderness tend to have lower strength.

The core test is another method for testing concrete compressive strength. In this test, a concrete core is taken from the structure (Figure 2.2), and the maximum compressive strength is determined by subjecting the core to a compressive load. The core test provides a more accurate measure of in-situ concrete strength but can be time-consuming and costly.

The rebound hammer (or "Schmidt hammer") test is a Non-Destructive Testing (NDT) method used to estimate concrete compressive strength. In this test, a rebound hammer is used to measure the rebound of a steel ball after striking the concrete surface (Figure 2.3). The rebound value is then correlated to a compressive strength value. The rebound hammer test is a quick and easy method of testing, but it can be affected by surface irregularities and does not provide an accurate measure of in-situ concrete strength (Shariati et al., 2011).

The maturity test is another commonly used method to evaluate early age concrete hydration via monitoring the temperature difference of concrete. The premise of this method is that the concrete strength gain is attributed to the exothermal chemical reaction of cementitious materials (e.g., cement, supplementary materials)

Figure 2.1 A typical compression testing setup.

Figure 2.2 A typical core drilling setup (Ju et al., 2017).

and water. The maturity method utilizes temperature history to correlate the strength gain of concrete. The standard ASTM C1074 provides an instruction (Figure 2.4) of a procedure to evaluate concrete strength using the maturity method. The maturity test is relying on established strength-maturity curves in the laboratory for application. The laboratory results always have considerable variation compared with the results obtained from the in-situ field due to the influence of ambient temperature. Also, it needs to be calibrated each time the concrete mix change. Therefore, it is inconvenient for field implementations.

In summary, core drilling has the advantage of higher accuracy but has lower efficiency; rebound hammer has the advantage of easier operation but has lower accuracy. The maturity method requires calibration of maturity index to each concrete mix, so it is inconvenient. Currently, the hydraulic compression testing is still the most commonly accepted method for concrete strength testing because of its simplicity and cost-effectiveness, despite its results can be influenced by various factors, such as the specimen geometry, fabrication process, loading speed etc.

2.2 Stress Wave Based Testing Methods for Mechanical Properties of Concrete

2.2.1 Metric Selection and Method Classification

To measure the mechanical properties of concrete, various physical metrics are reviewed and listed in Figure 2.5. The acoustic or ultrasound methods use the mechanical wave to probe the in-place dynamic modulus of concrete. This category of methods includes Impact Echo (IE), Impact Resonance (IR), Ultrasonic Pulse Velocity (UPV), Electro-Mechanical Impedance Spectroscopy (EMI), and Surface Acoustic Wave (SAW). The extent of disturbance (particle displacement) on the solid material caused by mechanical waves is determined by mechanical properties of the material, such as the density, dynamic modulus, viscosity, etc. Therefore, the acoustic or ultrasonic methods are naturally related to the objective of this study. The optical or electromagnetic methods use the light or electromagnetic wave as the probe signal. This category of methods includes optical fiber and Ground Penetration Radar (GPR). The hydration (hardening) process of concrete not only results in the gaining of elastic modulus and strength, but also reduces the water content, which influences the propagation of electromagnetic wave in concrete. Therefore, the optical or electromagnetic wave method is only suitable for monitoring the relative change of the concrete properties rather than measuring the absolute value. The thermal category includes the maturity method, which is specified for strength monitoring in ASTM C1074. Maturity method uses the accumulated hydration heat as the probe metric, which is related to the strength gaining of concrete. However, extensive calibration is required to build the correlation between this metric and the target value, and such calibration needs to be done for each specific concrete mixtures. Therefore, this method is useful but inefficient. The electrical category includes the electrical resistivity method. Like electromagnetic method, it monitors of the change of water content during hydration process rather than directly measuring the mechanical properties of concrete. In summary, the acoustic signal is the metric that is closer to the target value to be measured regarding the physics similarity. Following sections will introduce the application of various acoustical methods in concrete mechanical properties monitoring.

2.2.2 Impact Echo Method

Impact Echo (IE) is a non-destructive testing method that has been utilized in the field of engineering for decades. The IE method was first developed by the National Institute of Standards and Technology (NIST) and Cornell University in 1986 as a nondestructive testing technique specifically for concrete applications (Carino et al., 1986). It is a low-frequency elastic-wave method based on the transient response of a member to mechanical impact. There are a number of

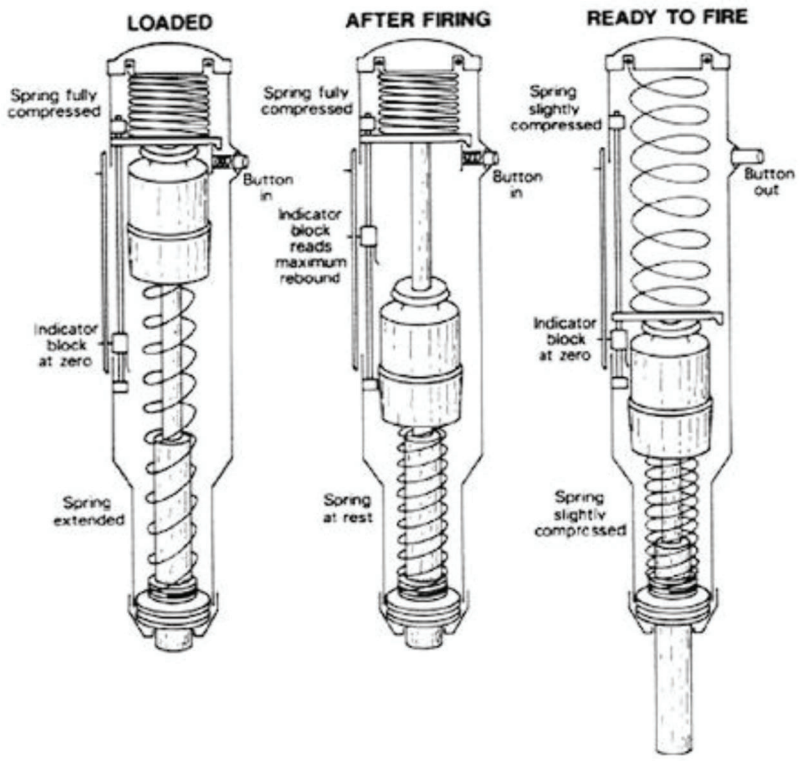

Figure 2.3 Rebound hammer (Shariati et al., 2011).

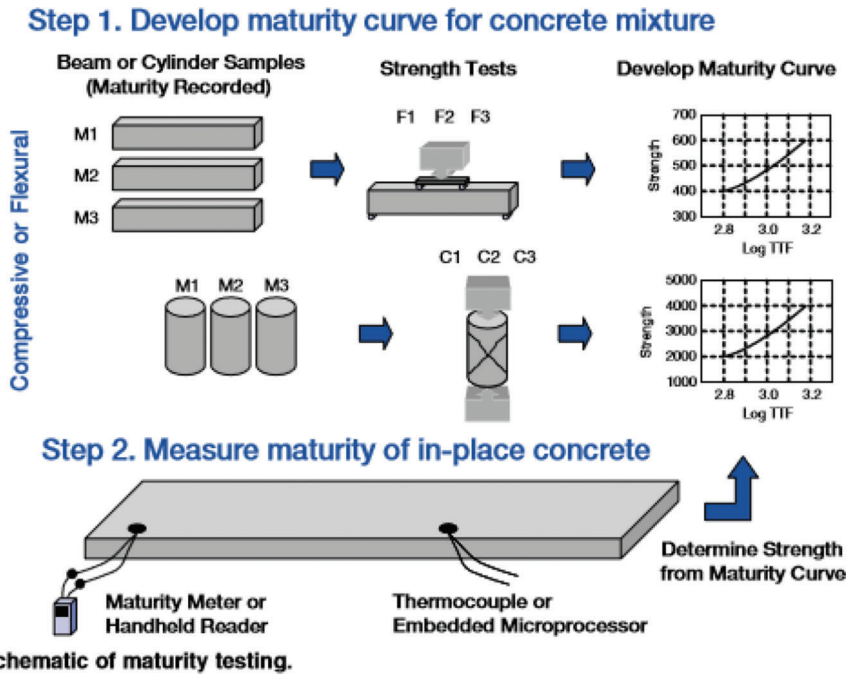

Figure 2.4 Maturity testing (FHWA, 2005).

situations where the IE method has proven applicable, including thickness measurement of slabs and cylinder walls (Sansalone, 1997). The technique is also used to detect flaws in a wide variety of materials, such as concrete and masonry (Cheng & Sansalone, 1993; Sadri, 2003). The theoretical study on IE method revealed that the impact echo resonance in the thickness direction of a plate is corresponding to the Zero-Group-Velocity (ZGV) frequency of the S1 Lamb wave mode (Figure 2.6) and explained the basis of the correction factor that was previously used as an empirical number (Gibson & Popovics, 2005).

Acoustic / Ultrasonic
Impact Echo
Impact Resonance
Ultrasonic Pulse Velocity
Electro-mechanical Impedance Spectroscopy
Surface Acoustic Wave

Optical / Electromagnetic
Optical Fiber
Ground Penetration Radar (GPR)

Thermal
Maturity Method

Electrical
Electrical Resistivity

Figure 2.5 Testing methods using various physical metrics.

2.2.3 Impact Resonance Method

The Impact Resonance (IR) test is a nondestructive test method that is used to characterize the dynamic modulus of concrete. The IR test method induces an excitation by striking a mass, usually a steel ball, onto a test specimen and measuring the natural vibration of the specimen, which can then be used to determine the specimen's material properties. This method is preferred over the traditional axial compression modulus method because the setup of the IR test is simpler, more efficient, and less expensive than standard. This method has been specified in ASTM C215. Researchers also explored its application in other materials like the asphalt and asphalt concrete (Ryden, 2011). Although the IR method can be used to measure the dynamic modulus, it needs to be noted that the dynamic modulus and static modulus are two related but very different material properties. The static modulus of concrete has been demonstrated to be more dependent on the elastic properties of the cement paste, whereas, for stress wave methods like IR method and the ultrasonic pulse velocity method in the next section, the dynamic modulus is more dependent on the elastic properties of the aggregates. Literature (Lee et al., 2017) compared the dynamic-static modulus empirical correlations and the Figure 2.7 shows the variation of such correlation is not neglectable.

2.2.4 Ultrasonic Pulse Velocity

Ultrasonic Pulse Velocity (UPV) is based on the propagation of ultrasonic waves through the material and measuring the Time of Flight (TOF) of the waves. The TOF is then used to calculate the velocity of the waves and thus the elasticity of the material. Obviously if the concrete has more pores, cracks or poor quality, the ultrasound velocity will be slower, so it can be used as a flaw detection method. UPV has been specified in ASTM C 597, however, in the standard it is explicitly clarified that UPV is "not to be considered as a means of measuring strength nor as an adequate test for establishing compliance of the modulus of elasticity of field concrete with that assumed in the design. The longitudinal resonance method in Test Method C215 (ASTM, 2019) is recommended for determining the dynamic modulus of elasticity of test specimens." Nevertheless, literature has reported applications of UPV on concrete strength and dynamic modulus testing (Al-Nu'man et al., 2015; Diaferio & Vitti, 2021; Kewalramani & Gupta, 2006; Mahure et al., 2011; Trtnik et al., 2009). The formulas that convert the UPV to concrete strength varies according to material compositions, so its limitation is similar to IE and IR, i.e., the conversion from dynamic mechanical properties to static properties. Another limitation of UPV method is that a pair of ultrasound transducers are required for its setup (see Figure 2.8) and such transducers are expensive, so their application is limited to surface mounting setup or small size specimen through-transmission testing.

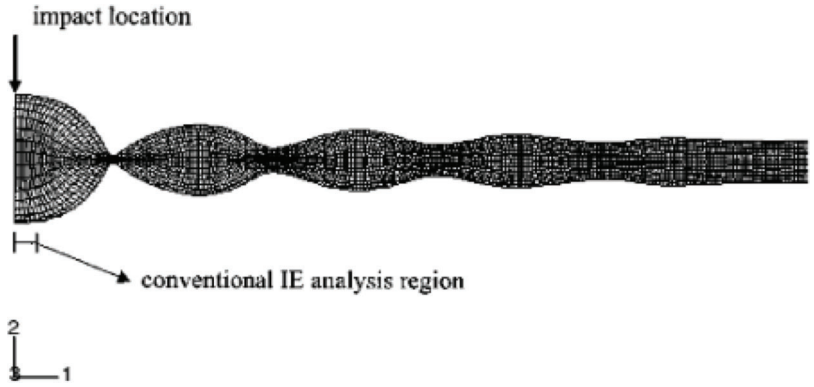

Figure 2.6 Vibration mode shape of IE resonance of a slab (Gibson & Popovics, 2005).

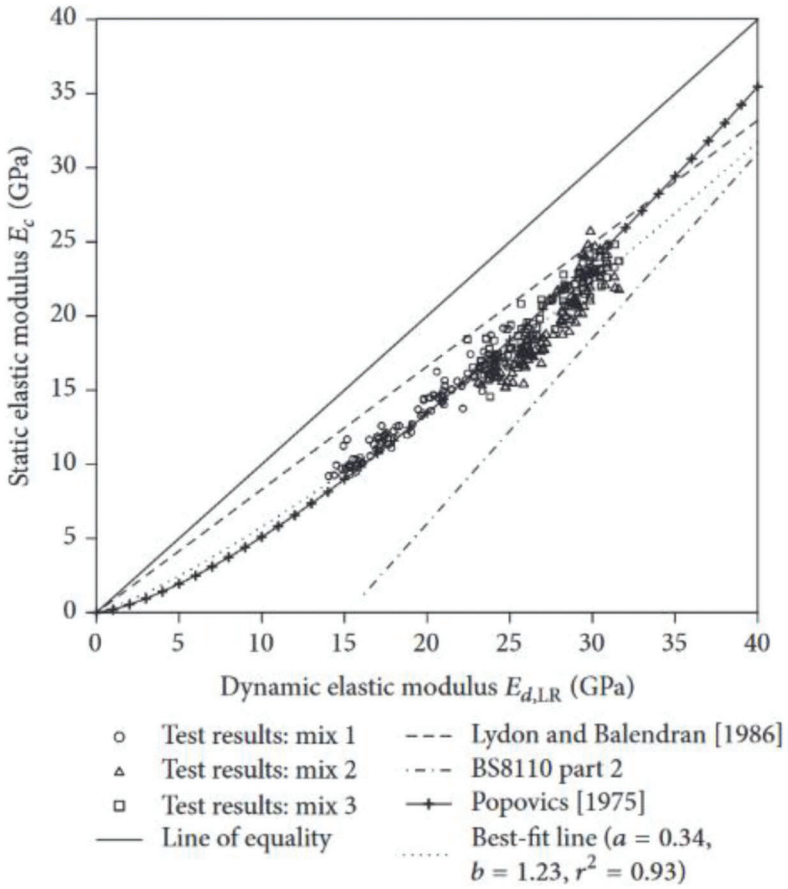

Figure 2.7 Static-dynamic modulus empirical correlation curves (Lee et al., 2017).

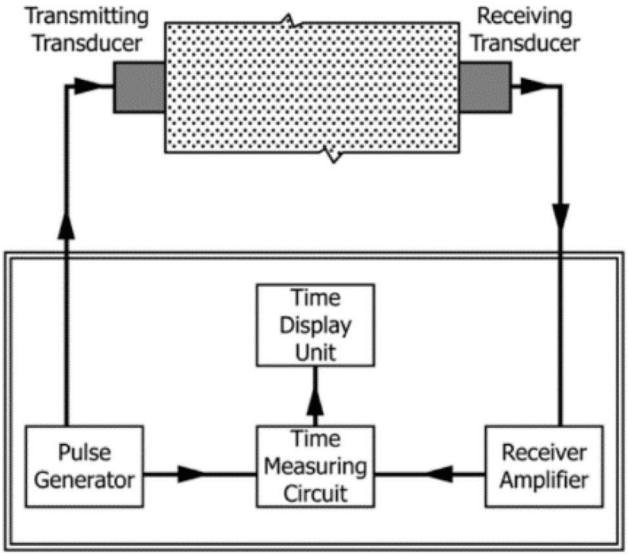

Figure 2.8 UPV testing setup (ASTM C597).

2.2.5 Electro-Mechanical Impedance Spectroscopy (EMI)

The EMI method is also classified as one of the stress-wave based sensing methods, but it is distinct from most of other stress-wave based methods in several aspects, including both advantages and limitations. The advantage of existing EMI methods for concrete strength monitoring purpose is that this method only involves one single piezoelectric sensor and one combined transmission-receiving process, which enables easier testing setup and lower hardware cost. Traditional stress-wave based methods (like UPV) either (1) require a pair transducers to work as the transmitter and the receiver separately; or (2) use a single transducer but the transmission process and receiving process are separate in time, and usually an electrical relay (or "T-R switch") is needed to change the operation mode of such transducer (Carpenter et al., 2018). On the other hand, the limitation of the existing EMI sensing methods for concrete strength monitoring includes (1) current studies lack the understanding of sensing area of EMI sensors and (2) the understanding of the physical interaction between concrete mechanical properties and the EMI signal is limited to "effective mechanical impedance" (Ballah & Soh, 2004a). Although mathematical and numerical models were reported in literature (Ballah & Soh, 2004a; Liang et al., 1994; Narayanan et al., 2017; Wang et al., 2014), the influence of host structure (concrete) on the piezoelectric sensor is simplified as the mechanical boundary condition to the piezoelectric sensor, and few literature reported the study on the wave field problem, i.e., how

TABLE 2.1
Summary of Sensing Metric and Sensor Packaging Method

Literature	Signal Processing Metric		Sensor Packaging
	Spectrum Amplitude	Resonant Frequency	
Su et al., 2019	×		Conformal coating
Bhalla & Soh, 2004a	×		Conformal coating
Wang et al., 2014	×		Conformal coating
Narayanan et al., 2017	×		Conformal coating
Lu et al., 2018		×	Bonding PZT on a metal strip
Luo et al., 2010		×	Bonding PZT on a metal block
Providakis & Liarakos, 2011		×	Bonding PZT on a Teflon enclosure

such boundary condition is formed and influenced by the host structure material surrounding the sensor. Literature (Fan et al., 2018; Yang & Divsholi, 2010) studied the sensing distance of EMI sensors for impact damage and saw cut damage and reported the sensing distance to be several tens of centimeters to half a meter. However, these studies are performed on fully cured concrete and may not be suitable to describe the sensing distance of EMI sensors in fresh concrete. Besides the understanding of the physical basis, the signal processing is another important part of EMI sensing technique. The signal processing metrics can be classified into two categories: the spectrum amplitude and the resonant frequency. The two metrics have different physical basis and therefore have different influence on the sensor packaging method. Specifically, the EMI methods those use spectrum amplitude as the metric are more sensitive to the damping caused by the sensor packaging material, so these methods require as less packaging to the piezoelectric element as possible. For example, literature (Saravanan et al., 2015) introduced a packaging method using cement block ("smart aggregate"), and found the signal is not sensitive to strength gaining in early age of concrete curing. In most applications, the piezoelectric element is coated with conformal material like a thin layer of epoxy. In contrast, the EMI methods those use spectrum resonant frequency as the metric care more about the structure of the sensor and its vibration mode, so there is more flexibility on the sensor packaging designs. The summary of the sensing metric and sensor packaging method is show in Table 2.1.

3. IMPROVED EMI SENSORS AND SENSING SYSTEM

This chapter reports the work of using the novel EMI sensor and corresponding sensing system to monitor the strength of concrete. Theoretical models describing how to measure the resonant frequencies of concrete through EMI spectrum are introduced. FE simulation is also used to demonstrate the mechanism of the sensing process. Then, such theory is validated through embedding piezoelectric sensors in concrete cylinders. The development of the miniaturized impedance analyzer with wireless transmission function is also introduced in this part.

3.1 Improved EMI Sensor and Sensing Mechanism

3.1.1 Measurement of Concrete Resonance Using a Single Sensor

The physical model of EMI admittance originated from Liang's 1D model (Liang et al., 1994). Bhalla and Soh (2004a) developed the 2D effective EMI model. For the thin plate-like PZT patch the model of Bhalla is reasonable to describe the interaction between a host structure and a PZT sensor.

The electrical admittance amplitude of PZT is:

$$\bar{Y} = 4\omega j \frac{l^2}{h}\left[\overline{\varepsilon_{33}^T} - \frac{2d_{31}^2\overline{Y^E}}{(1-v)} + \frac{2d_{31}^2\overline{Y^E}}{(1-v)}\left(\frac{Z_{a,eff}}{Z_{a,eff}+Z_{s,eff}}\right)\overline{T}\right] \quad \text{(Eq. 3.1)}$$

where $\bar{Y}$ is electrical admittance; ω is the angular frequency; l is half of the PZT length; h is the thickness of PZT; $\overline{\varepsilon_{33}^T} = \varepsilon_{33}^T(1-\sigma j)$ is the complex dielectric permittivity at constant stress; d_{31} is piezoelectric constant; v is the Poisson's ratio of PZT; $\overline{Y^E} = Y^E(1+\eta j)$ is the complex Young's modulus of PZT; σ denotes the dielectric loss factor and η the mechanical loss factor; $Z_{a,eff}$ and $Z_{s,eff}$ are the effective mechanical impedance of PZT and host structure, respectively; $\bar{T} = \frac{\tan C_{\kappa l}}{C_{\kappa l}}$ is the correction factor, C is constant, $\kappa = \omega\sqrt{\frac{\rho(1-v^2)}{\overline{Y^E}}}$ is the wave number of PZT, ρ is the density of PZT.

The effective mechanical impedance of free PZT is given by

$$Z_{a,eff} = \frac{2h\overline{Y^E}}{j\omega(1-v)\bar{T}} \quad \text{(Eq. 3.2)}$$

As derived in (Bhalla & Soh, 2004a), the displacements of the PZT patch in the two principal directions are given by

$$u_1 = (A_1 \sin C\kappa x)e^{j\omega t} \quad \text{(Eq. 3.3)}$$

$$u_2 = (A_2 \sin C\kappa x)e^{j\omega t} \quad \text{(Eq. 3.4)}$$

where A_1 and A_2 are given by

$$A_1 + A_2 = \frac{2d_{31}V_0}{(\cos C\kappa l)C\kappa h}\left(\frac{Z_{a,eff}}{Z_{a,eff}+Z_{s,eff}}\right) \quad \text{(Eq. 3.5)}$$

Assuming the PZT patch vibrates in the same way in two directions, i.e., $A_1 = A_2$, and the amplitude of excitation voltage $V_0 = 1.0\ V$, the displacement amplitude of PZT in one direction is

$$u_1 = \frac{d_{31}\bar{T}l}{h}\left(\frac{Z_{a,eff}}{Z_{a,eff}+Z_{s,eff}}\right) \quad \text{(Eq. 3.6)}$$

The velocity amplitude of PZT in one direction is

$$\dot{u}_1 = j\omega u_1 \quad \text{(Eq. 3.7)}$$

Therefore

$$\frac{\partial \dot{u}_1}{\partial \omega} = j\cdot\frac{d_{31}l}{h}\cdot\frac{\partial}{\partial\omega}\left(\frac{\omega\cdot\bar{T}\cdot Z_{a,eff}}{Z_{a,eff}+Z_{s,eff}}\right) \quad \text{(Eq. 3.8)}$$

The derivative of electrical admittance of PZT to angular frequency is given by

$$\frac{\partial \bar{Y}}{\partial \omega} = 4j\cdot\frac{l^2}{h}\cdot\left[\overline{\varepsilon_{33}^T} - \frac{2d_{31}^2\overline{Y^E}}{(1-\nu)} + \frac{2d_{31}^2\overline{Y^E}}{(1-\nu)}\cdot\frac{\partial}{\partial\omega}\left(\frac{\omega\cdot\bar{T}\cdot Z_{a,eff}}{Z_{a,eff}+Z_{s,eff}}\right)\right] \quad \text{(Eq. 3.9)}$$

Equation 3.8 and Equation 3.9 can be rewritten as

$$\frac{\partial u_1}{\partial \omega} = L\cdot\frac{\partial}{\partial\omega}\left(\frac{\omega\cdot\bar{T}\cdot Z_{a,eff}}{Z_{a,eff}+Z_{s,eff}}\right) \quad \text{(Eq. 3.10)}$$

$$\frac{\partial \bar{Y}}{\partial \omega} = M + N\cdot\frac{\partial}{\partial\omega}\left(\frac{\omega\cdot\bar{T}\cdot Z_{a,eff}}{Z_{a,eff}+Z_{s,eff}}\right) \quad \text{(Eq. 3.11)}$$

where L, M, N are complex constants.

Comparing Equations 3.10 and 3.11, it can be seen that the electrical admittance of PZT has the same resonance behavior as the mechanical vibration of PZT and the resonance is caused by both $Z_{a,eff}$ and $Z_{s,eff}$.

If the frequency of interest is low, i.e., lower than $\frac{1}{5}$ of the first resonance frequency of PZT in free boundary condition, the $\bar{T} \approx 1$ (Bhalla & Soh, 2004a; Liang et al., 1994).

Then, Equation 3.2 can be rewritten as

$$Z_{a,eff} = \frac{2h\overline{Y^E}}{j\omega(1-\nu)} \quad \text{(Eq. 3.12)}$$

In such conditions, $Z_{a,eff}$ has a monotonic relationship with ω and it does not result in local maximums or minimums in $\frac{\partial \dot{u}_1}{\partial \omega}$ or $\frac{\partial \bar{Y}}{\partial \omega}$ The only factor that causes resonance of u_1 or $\bar{Y}$ is $Z_{s,eff}$, i.e., the mechanical impedance of the structure. Equation 3.10 through Equation 3.12 justified the reason EMI spectrum can be used to evaluate the velocity spectrum and evaluate the vibration modes of a concrete cylinder.

3.1.2 Validation of Concept on Concrete Cylinders

To validate the concept of measuring the mechanical resonance of host structure using the piezoelectric sensor's EMI spectrum, concrete cylinders (3 inches by 6 inches) were used as the host structure, and the piezoelectric sensor made of tubular PZT and epoxy potting material was embedded in such cylinders (shown in Figure 3.1 and Figure 3.2). The concrete was cured more than 28 days, so its mechanical properties have been stable. The standard IR test was performed on the cylinder according to ASTM C215 (Figure 3.3), then the same cylinder was used for EMI spectrum measurement (Figure 3.4). The IR results were plotted in Figure 3.5. The EMI spectrum was processed to show the derivative of the conductance to frequency for better visualization of the peaks Figure 3.6. The resonant peaks tested by IR and EMI method are reasonably close, so the concept is proved.

3.1.3 Modal Analysis of the Operation Mode of EMI Sensor

The FE simulation was performed to demonstrate how the localized resonance work. The FE was implemented using COMSOL (COMSOL, Inc. Stockholm, Sweden). The simulation is based on 2D axisymmetric assumption, in which the geometry, loadings, boundary conditions and materials are symmetric with respect to an axis is one that can be solved as an axisymmetric problem instead of as a 3D problem. The geometry of the simulation model is shown in Figure 3.7. The grey color area represents the concrete. The white color gap inside the concrete represents the waveguide of the sensor. The ideal waveguide material is just vacuum, so there is no material designated to the gap. The blue area is the Region of Interest (ROI) of concrete, which is expected to be excited by the sensor. There is no boundary condition set for the concrete except the axisymmetric axis because the modal analysis and frequency steady state analysis are not intended to search the global vibration mode of the concrete structure, instead these analyses are performed to study the vibration mode of the ROI.

To study whether the vibration mode of ROI is dependent on the host structure size, three widths (6 inches, 12 inches, and 24 inches) of the concrete structure were simulated. The outputs of modal analysis are the natural frequencies and the average velocity magnitudes of ROI at each natural frequency, so we can investigate at which natural frequency the ROI has the biggest response. The modal analysis results are shown in Figure 3.8. No matter the size of concrete structure, there exists a "standing" vibration mode around 32.5 kHz–33.0 kHz. Such mode is due to the localized resonance of ROI rather than the resonance of other

parts of the concrete. Figure 3.9, Figure 3.10, and Figure 3.11 present the mode shape at three different natural frequencies, and the "standing" vibration mode in Figure 3.10 corresponds to the localized resonance of ROI, as shown in Figure 3.8. To further demonstrate the function of the waveguide, or the white color gap in the concrete model in Figure 3.7, a simulation was performed to get the sensor's steady state response in frequency domain from 10 kHz to 50 kHz.

The localized resonance is somehow abstractive, so the wave field expressed in the logarithm velocity magnitude is visualized in Figure 3.12, Figure 3.13, and Figure 3.14. It is observed that the wave field has the largest excited area when the sensor reaches the resonant frequency. The prototype of the sensor and datalogger is shown in Figure 3.15 and Figure 3.16, respectively.

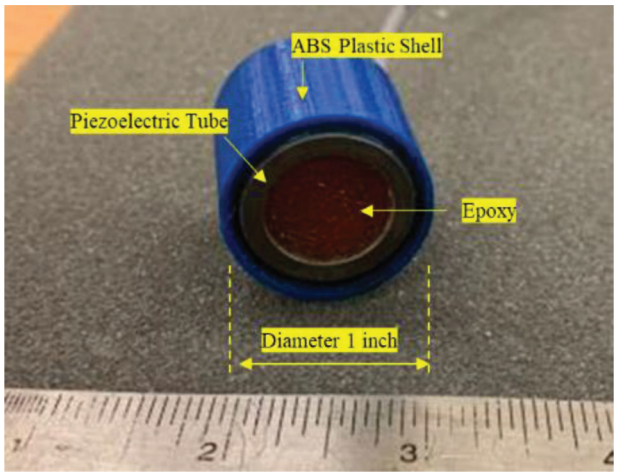

Figure 3.1 A sensor used for the validation test.

3.2 On-Chip Impedance Analyzer and Wireless Transmission

The wireless data transmission system was evolved in three versions: the teeny-tiny version, the blue tooth hub version, and the LTE version (current version).

The testing performance of LTE version datalogger, such as the frequency range and resolution, are as good as the expensive commercial analyzer. EMI spectrum measured using the datalogger match with commercial impedance analyzer. As shown in our previous work,

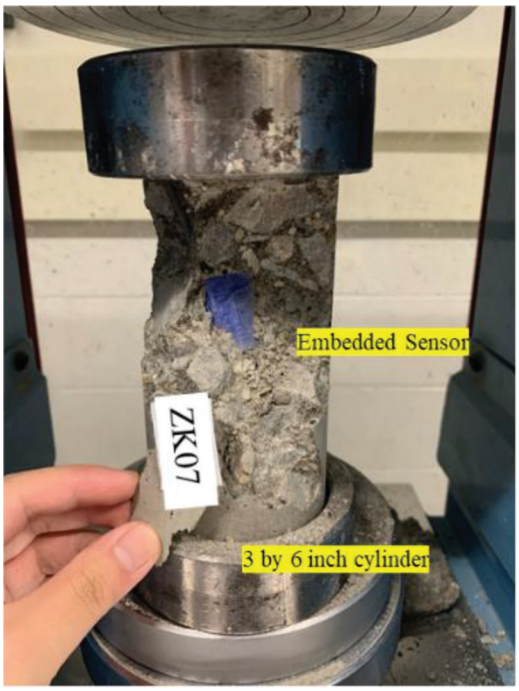

Figure 3.2 The position of the sensor in a concrete cylinder.

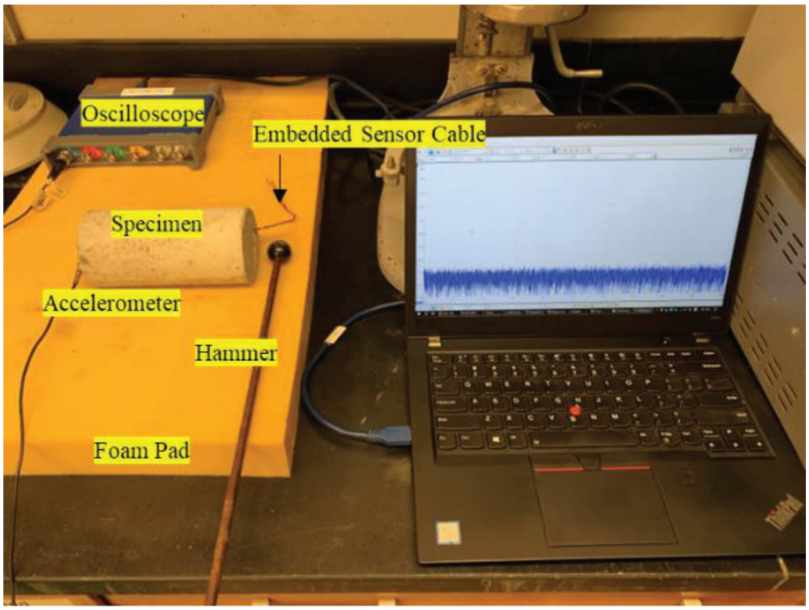

Figure 3.3 ASTM C215 testing setup.

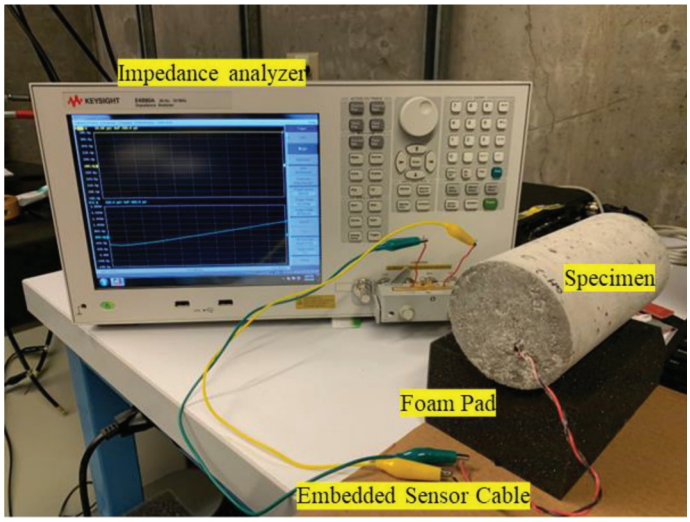

Figure 3.4 EMI spectrum testing setup.

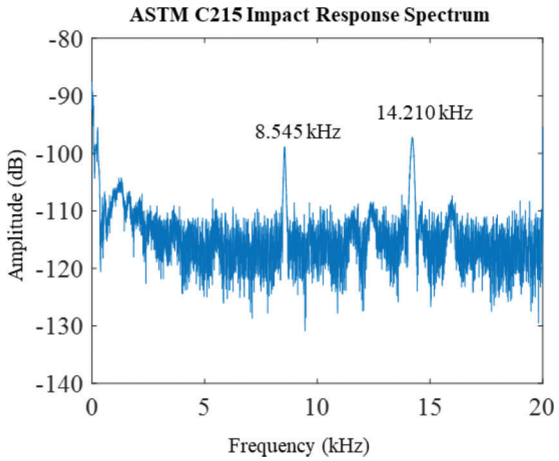

Figure 3.5 ASTM C215 testing result.

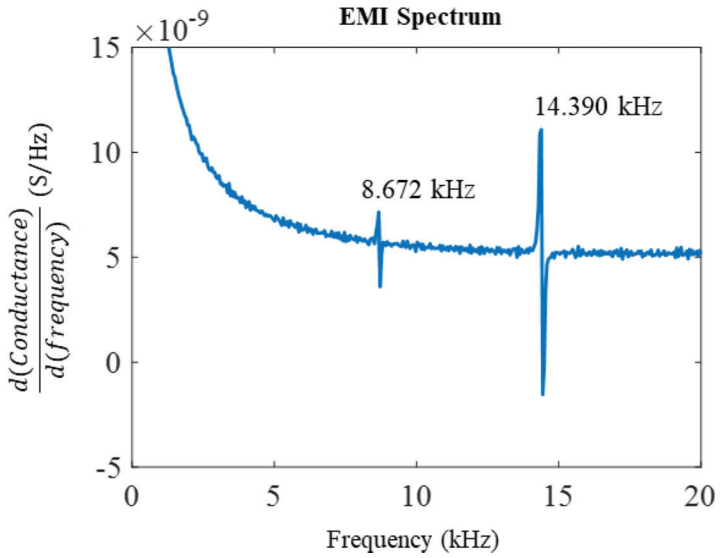

Figure 3.6 EMI sensor testing result.

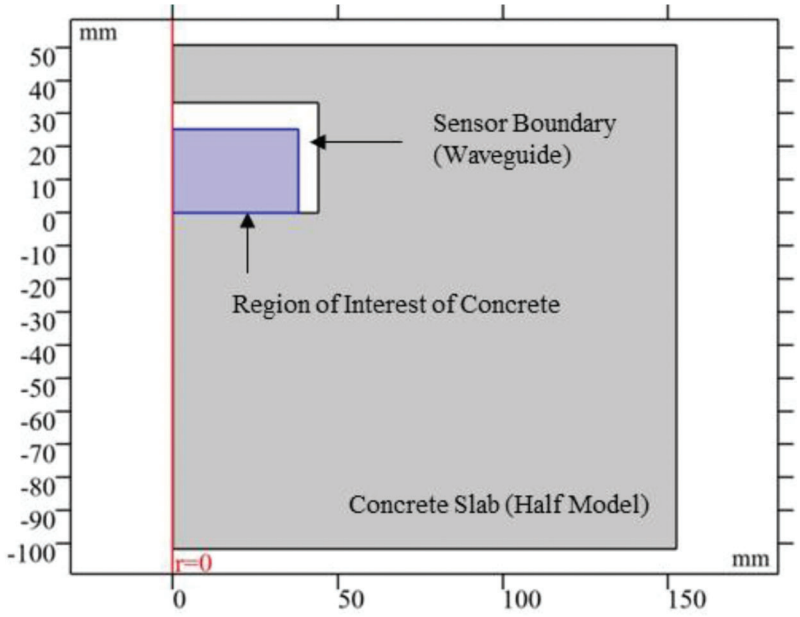

Figure 3.7 Simulation geometry model for modal analysis.

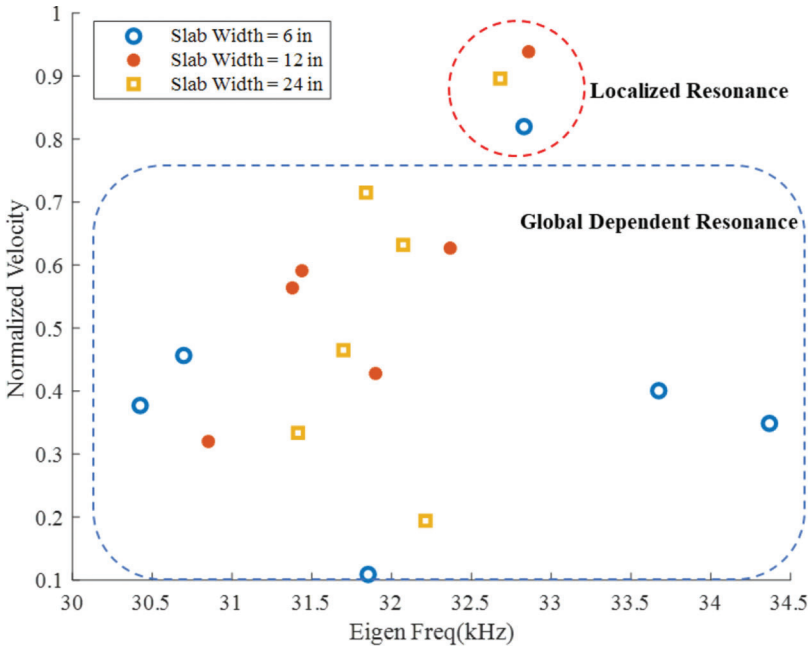

Figure 3.8 Modal analysis results of specimens with various sizes.

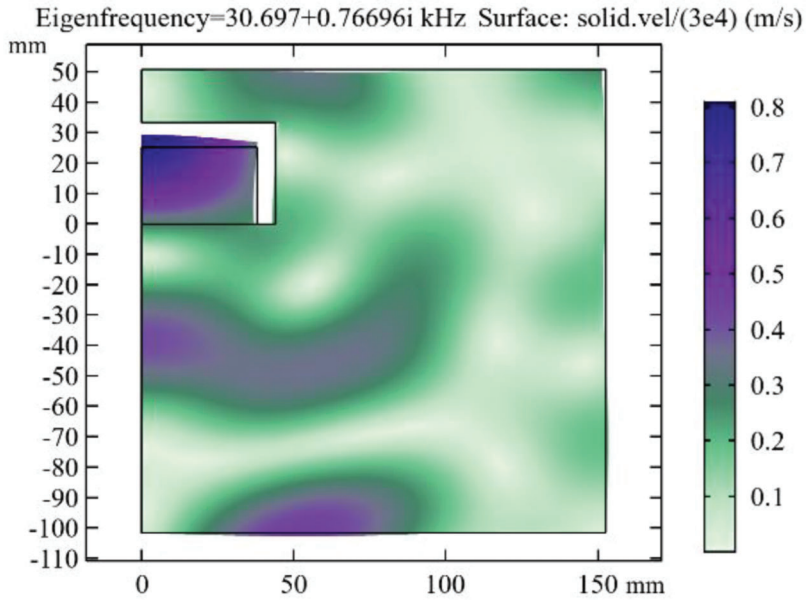

Figure 3.9 Vibration Mode 1 (Goble dependent).

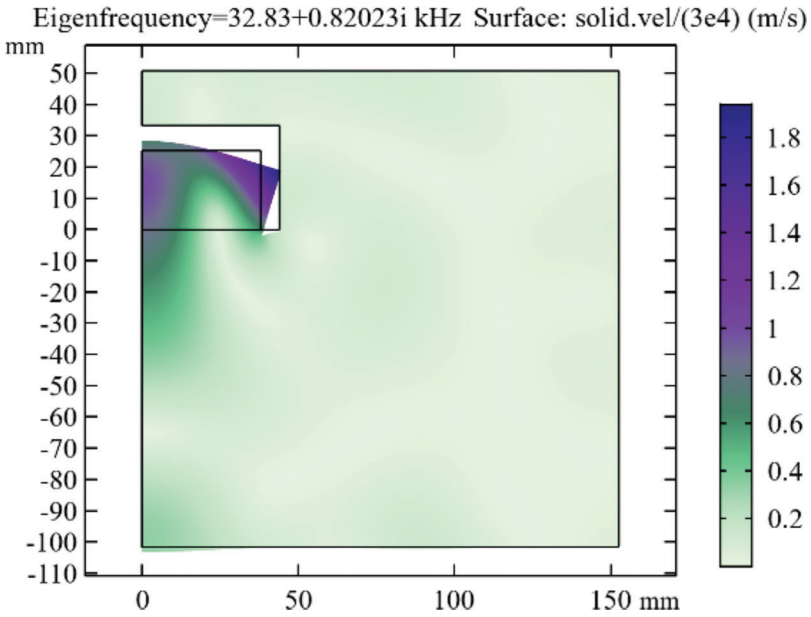

Figure 3.10 Vibration Mode 2 (Goble independent).

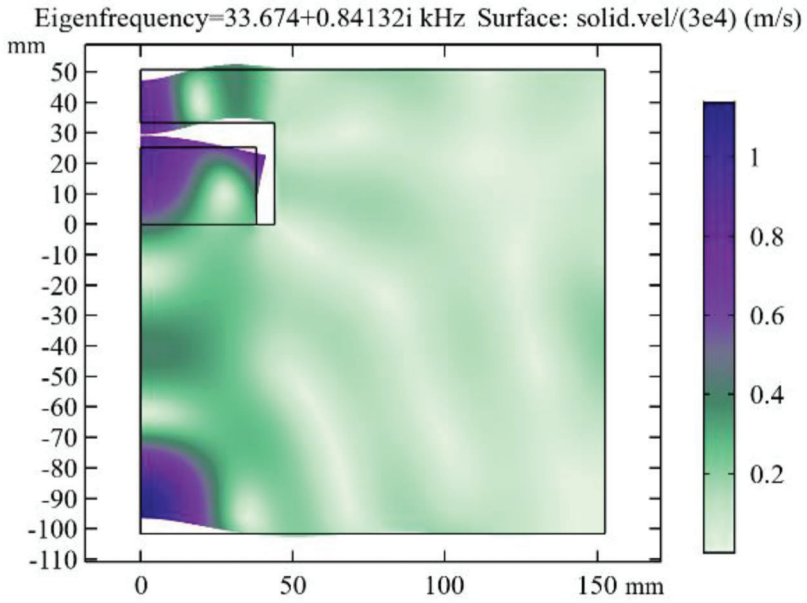

Figure 3.11 Vibration Mode 3 (Goble dependent).

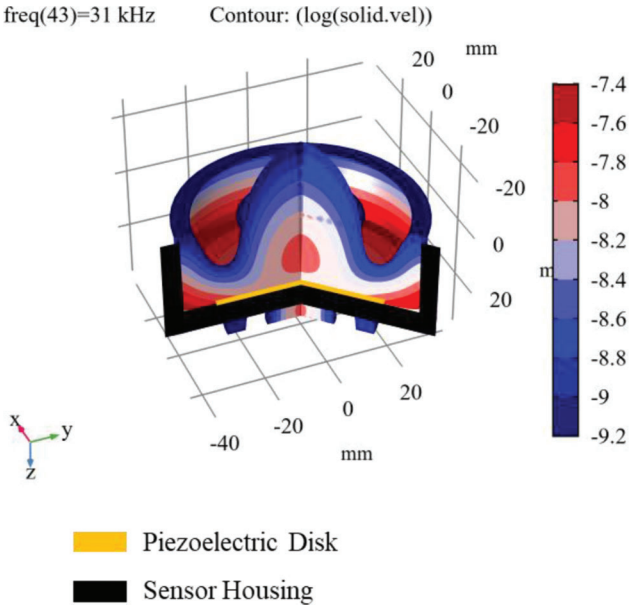

Figure 3.12 Sensor acoustic field at 31 kHz (off-resonant).

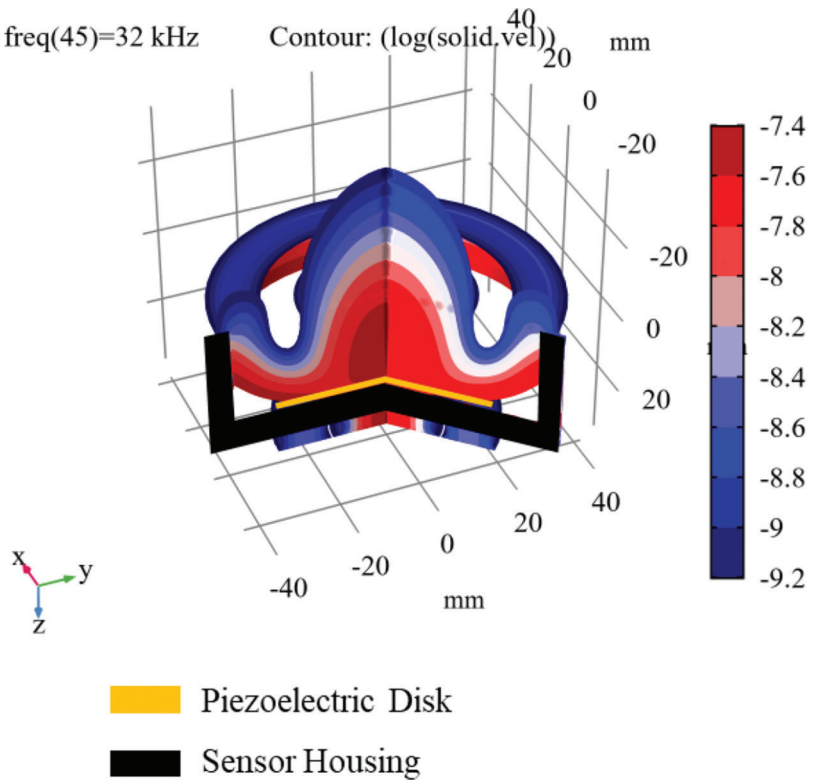

Figure 3.13 Sensor acoustic field at 32 kHz (resonant).

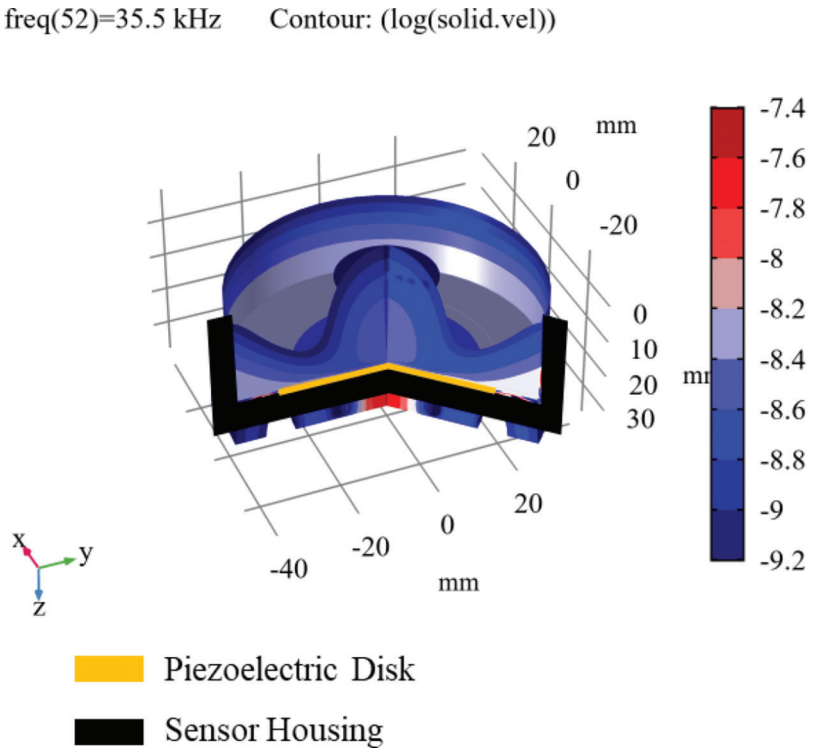

Figure 3.14 Sensor acoustic field at 35.5 kHz (off-resonant).

Figure 3.15 Finished prototype.

Figure 3.16 A sensor with the datalogger.

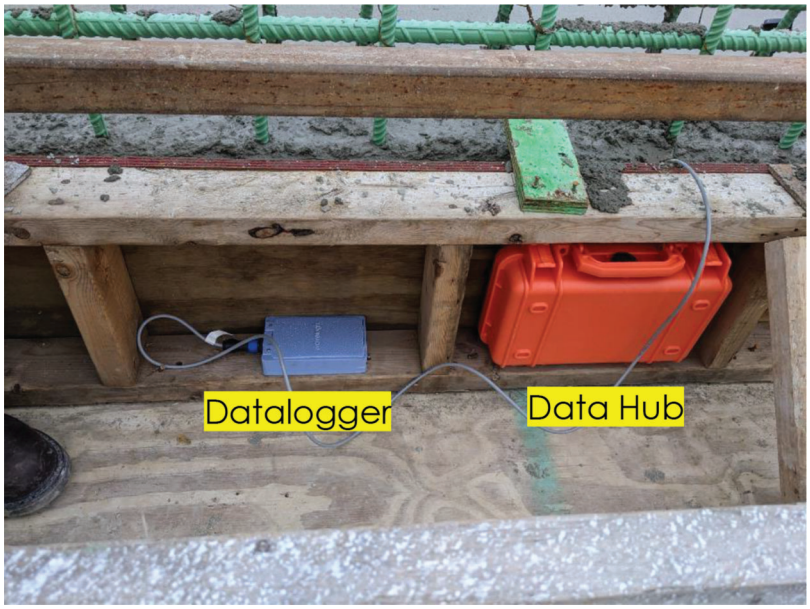

Figure 3.17 Datalogger with Bluetooth data hub.

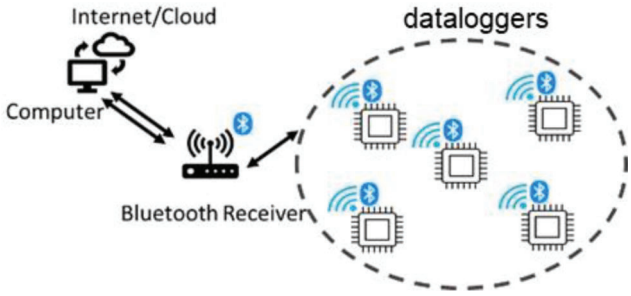

Figure 3.18 Data transmission of Bluetooth hub version datalogger.

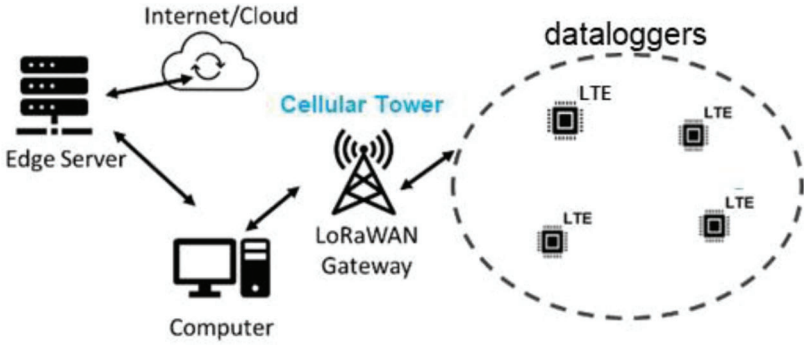

Figure 3.19 Data transmission of LTE version datalogger.

such spectra could be further processed to determine the concrete strength. The wireless data transmission schemes for Bluetooth version and LTE version were shown in Figure 3.17, Figure 3.18, Figure 3.19, and Figure 3.20. The data communication range of Bluetooth version datalogger is 65 feet, and the LTE version datalogger directly sends data via cellular towers. The research team developed a database along with front-end and back-end to visualize and manage the data.

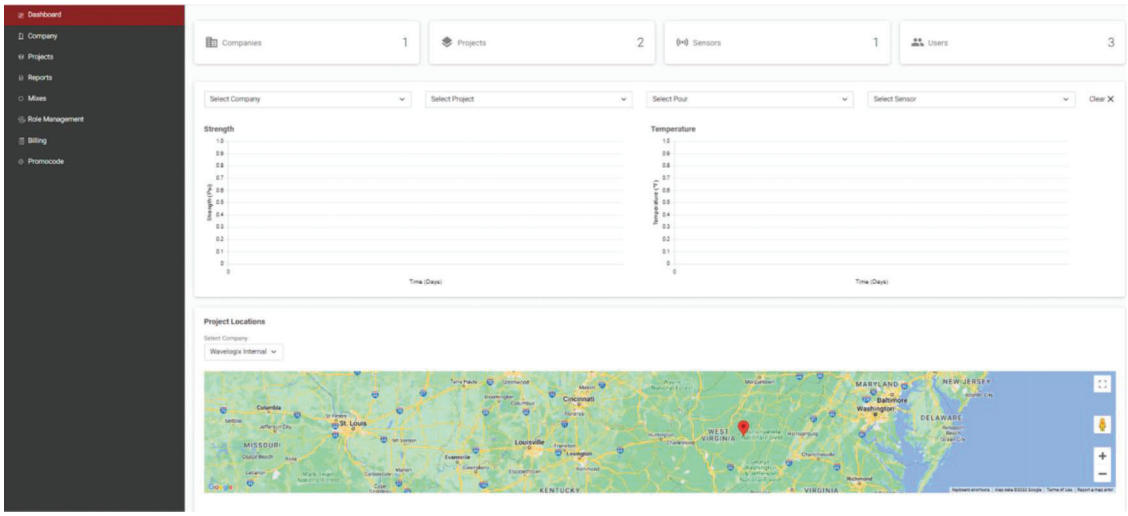

Figure 3.20 Dashboard of database management website.

4. LABORATORY TESTING

Although there exists a theoretical correlation between the resonant frequencies of EMI sensors and the dynamic elastic modulus of concrete (as introduced in Chapter 3), the correlation between the resonant frequencies of EMI sensors and the compressive strength of concrete is not determined yet. The ACI 318-19 specified a conversion function from static elastic modulus to the strength. The EMI spectrums are measured with compressive test conducted simultaneously at the age of interest to validate the EMI sensing result. Due to the conditions of laboratory scaled cylindrical samples are different from the large-scaled mass concrete, the concrete slab was also conducted in the lab testing work.

4.1 Mortar Testing for Consistency Study

The mechanism of EMI sensors is essentially based on stress-wave propagation in the host material. Concrete is a well-known inhomogeneous material which comprises of cementitious binder, fine aggregates, and coarse aggregates. In contrast, mortars comprising of the cementitious binder and fine aggregates, are more homogeneous than concrete. Therefore, the mortar is used to study the consistency of sensor signals measured by various sensors.

Ten sensors are embedded in five standard beam molds (6 inches by 6 inches by 22 inches), as shown in Figure 4.1. The sensors are first placed at the bottom of the molds, then the mortar is placed in the mold in three layers. A steel rod is used to consolidate the material carefully to avoid honeycomb or big voids.

The typical EMI spectrum measured by a sensor is presented in Figure 4.2. It can be observed that the resonant was weak at the first two spectrums. This is because the concrete was still in liquid stage when those two spectrums were measured, and liquid concrete has higher attenuation to the vibration of the sensor and dampens the spectrum peak. The resonant peak became sharper when time progresses. This is because concrete is gaining strength and the attenuation to the vibration of the sensor is decreasing. Figure 4.3 shows the resonant frequencies of the spectrums measured by 10 sensors in 90-hour period. The Coefficient of Variance (COV) of the resonant frequencies is plotted in the right y-axis. It can be seen that the trend of the resonant frequencies versus time is in a logarithmic shape, and the COV is less than 1.5% and stabilized at 1.1% when the mortar hydration is stabilized. Figure 4.4 is an alternative expression of the EMI sensor signal without manually extracting the resonant. The time and frequency are x-axis and y-axis, respectively, and the amplitude of spectrum is z-axis, which is represented by color map. From Figure 4.4, it can be observed that there exists a light color band, and such band is due to the resonance of the signal spectrum.

In conclusion, the improved EMI sensor has the more prominent signal feature (the resonant peak) compared to traditional plate shape piezoelectric sensor coated with polymers. Such feature is closely related to the hydration process of concrete and can be explained through vibration modal analysis in Chapter 3. The variation of resonant frequencies of 10 sensors is less than 1.5% COV for mortar material, indicating a good consistency of sensor spectrums.

4.2 Concrete Testing for Material and Curing Condition Study

Concrete is more complicated than mortar and paste due to the involvement of different sizes of aggregate and admixtures. Therefore, the research team conducted concrete testing both in lab and in field. A summary plot of the concrete testing is shown in Figure 4.5. The linear regression was calculated using the resonant frequencies of the sensor and the

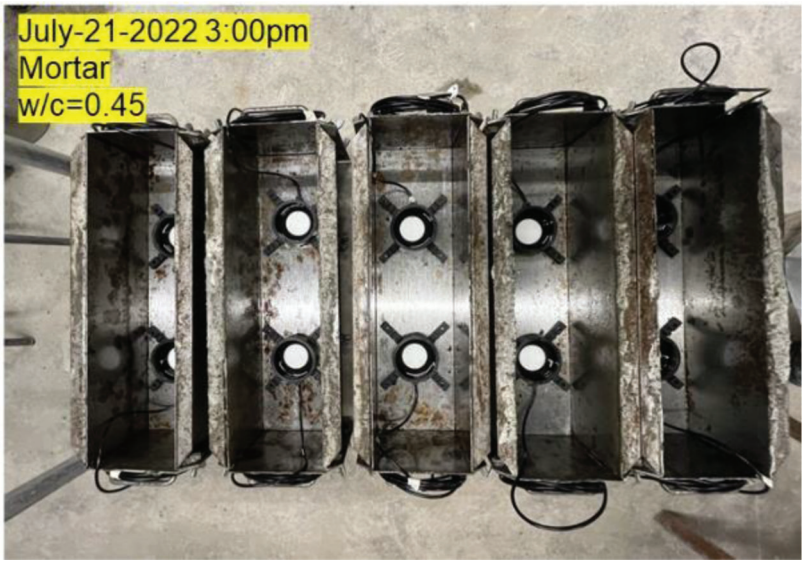

Figure 4.1 Sensor placement in beam molds.

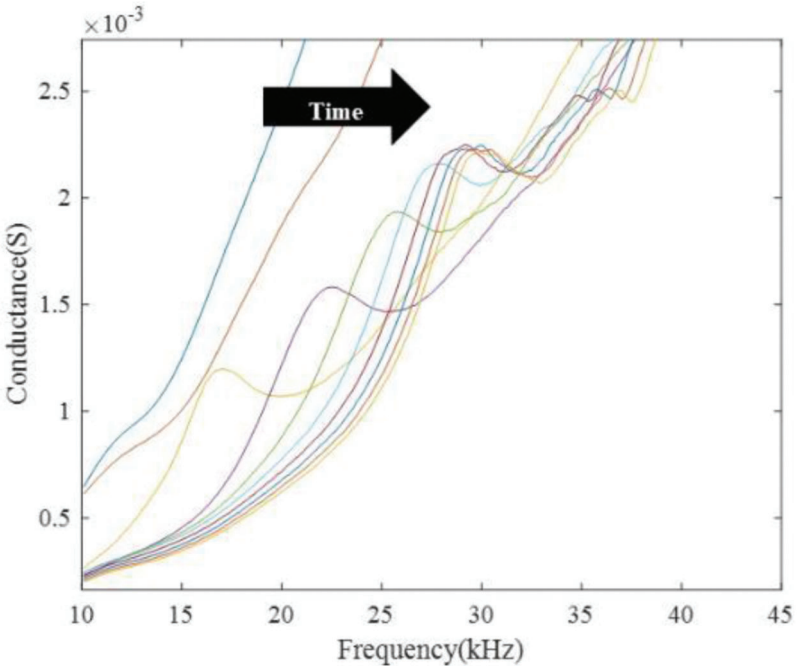

Figure 4.2 A typical sensor spectrum.

compressive strength of concrete cylinder. The regression was done for lab and field testing separately because the data collected in lab and in field are showing different correlations. The reason could be that the sensor resonant frequencies are influenced by other factors than the strength of concrete.

The concrete testing was firstly performed in a beam mold where three sensors were embedded in (Figure 4.6). The testing results are shown in Figure 4.7.

The concrete testing was also performed in a slab (3 feet by 3 feet by 8 inches). The purpose of this testing is to study the influence of the concrete sample size. As shown in Figure 4.8, five concrete beams and one slab were casted using the same batch of concrete. Two sensors were placed in one beam and five sensors were placed in the slab. The testing results are shown in Figure 4.9. The regression formula worked good for this testing, especially the COV is stabilized at 15%, which is comparable to the COV for cylinder compressive testing results threshold specified in ASTM C39.

The PLC cement is becoming prevalent in the concrete market to reduce carbon emission, so the research team also studied the influence of these two different cement types along with in lab (Figure 4.10)

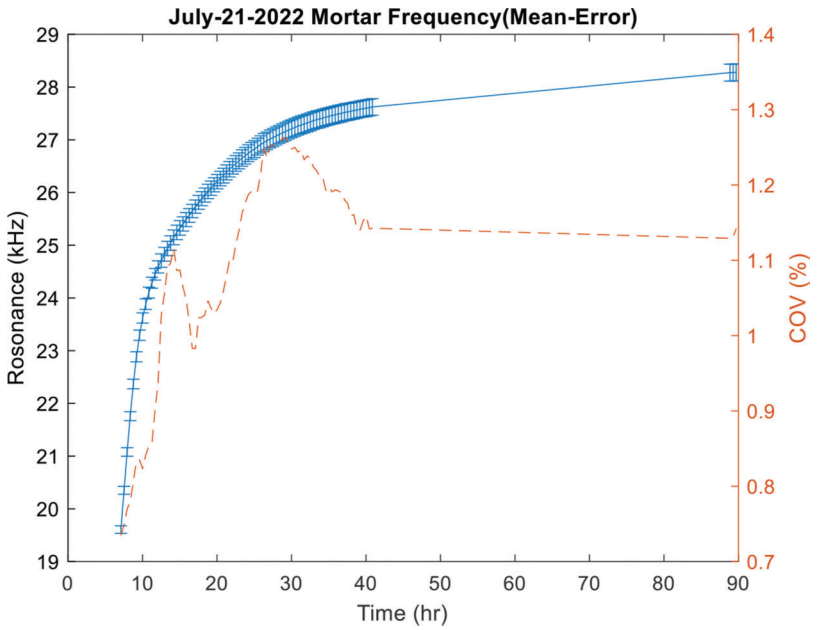

Figure 4.3 Resonant frequencies measured by sensors in mortar.

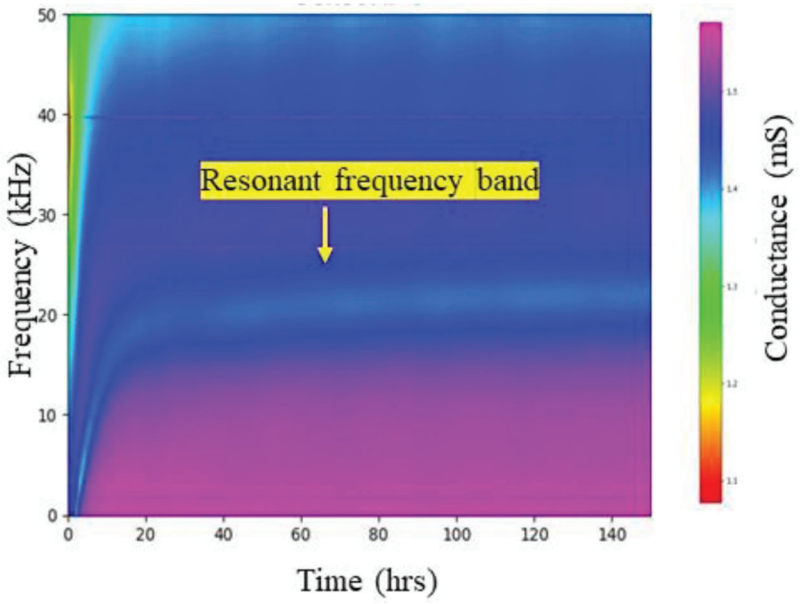

Figure 4.4 An alternative expression of sensor spectrum.

and outdoor (Figure 4.11) curing conditions. The outdoor curing condition is used to mimic the actual in field curing situation. The concrete mixture is the same other than the cement type. Testing results are shown in Figure 4.12, Figure 4.13, Figure 4.14, Figure 4.15, Figure 4.16, and Figure 4.17. For each group of testing, six sensors were embedded in two concrete beams (three in each), and three cylinders (3 inches by 6 inches) were compressed at each age as the reference points. In each figure, the mean value, max-min band, and the standard deviation band of six sensors and three cylinders are plotted. From the results we can observe that the OPC and PLC cement didn't cause significant difference in the sensor results, and the variation of sensor results is comparable to the variation of cylinder results. An interesting observation is that the sensor results of outdoor samples have some fluctuations and such fluctuations coincided with daily temperature change. This indicates that the sensor is subject to the influence of temperature change, though the extent of such influence is relieved when temperature recovers to normal domain around 70°F degree.

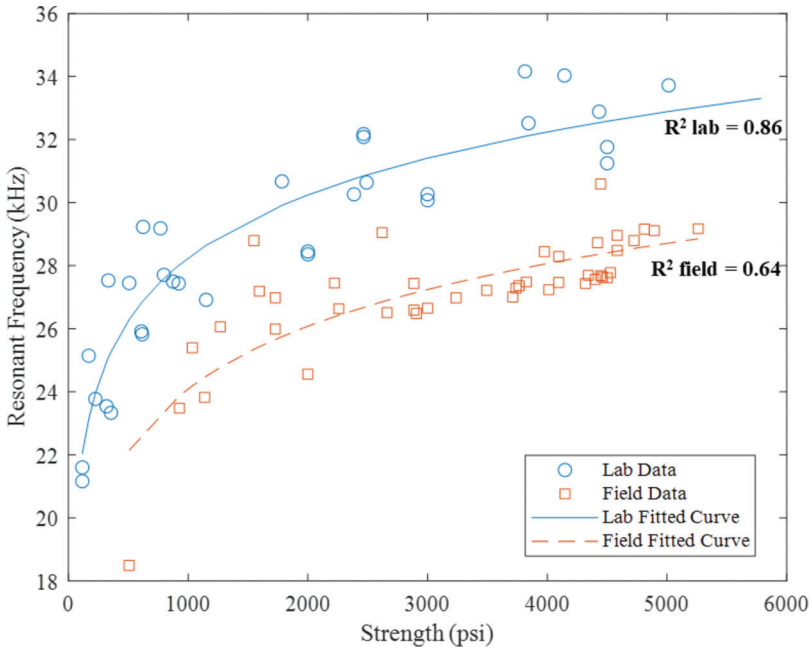

Figure 4.5 Regression curve of lab and field-testing data.

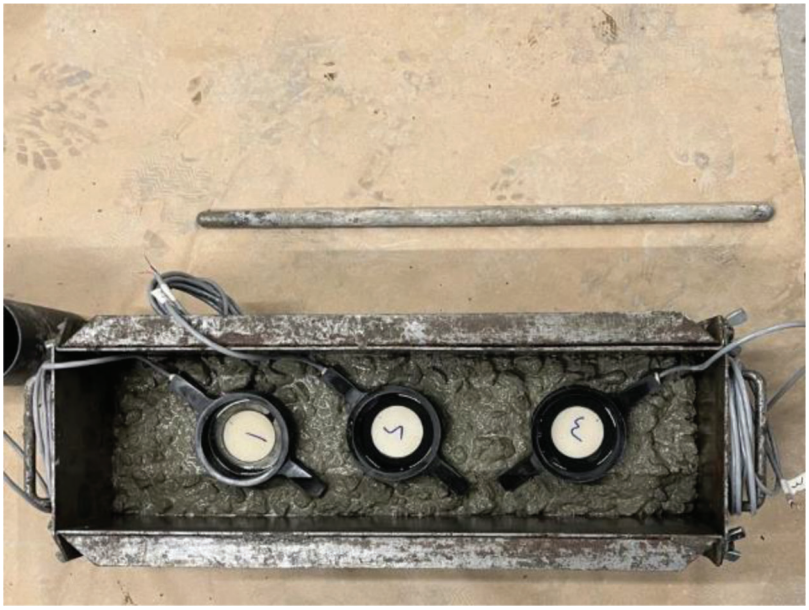

Figure 4.6 Sensor placement in concrete beam.

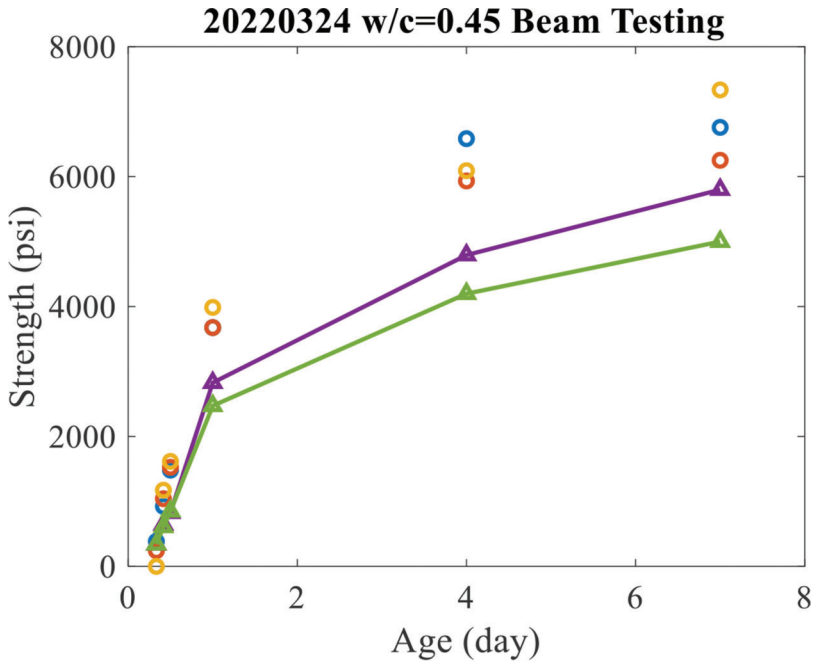

Figure 4.7 Testing results of sensors in the concrete beam.

Figure 4.8 Concrete beams and slab casted in the lab.

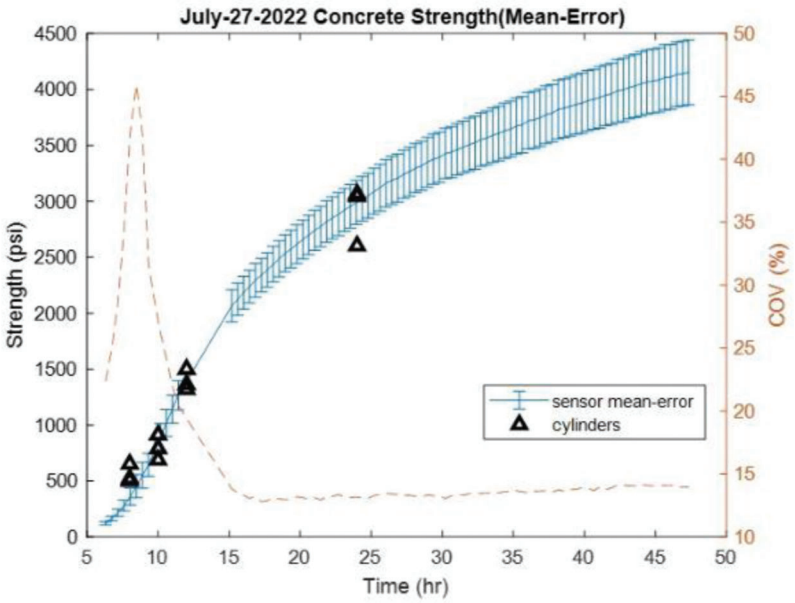

Figure 4.9 Testing results from sensors in beams and the slab.

Figure 4.10 Concrete samples cured outdoors.

Figure 4.11 Concrete samples cured in the lab.

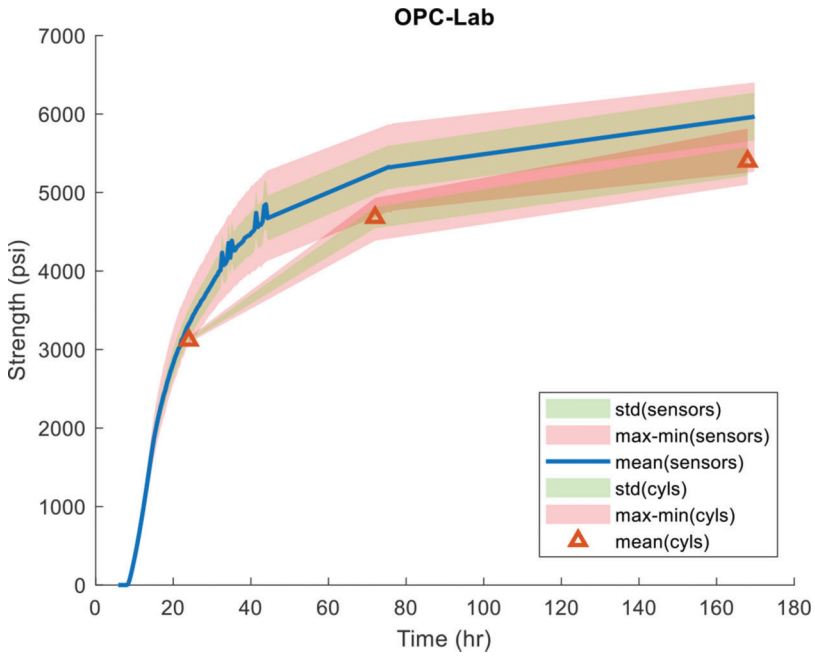

Figure 4.12 Testing results of sensors in OPC concrete cured in the lab.

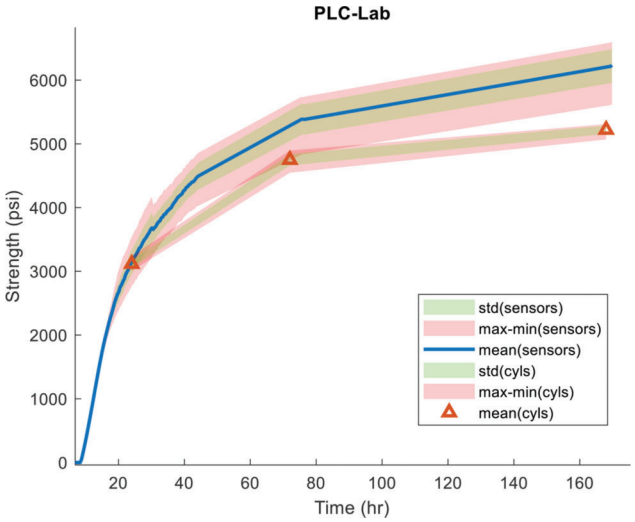

Figure 4.13 Testing results of sensors in PLC concrete cured in the lab.

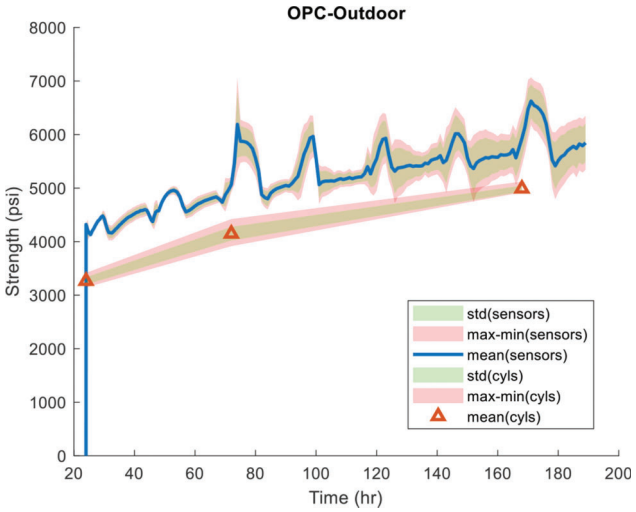

Figure 4.14 Testing results of sensors in OPC concrete cured outdoors.

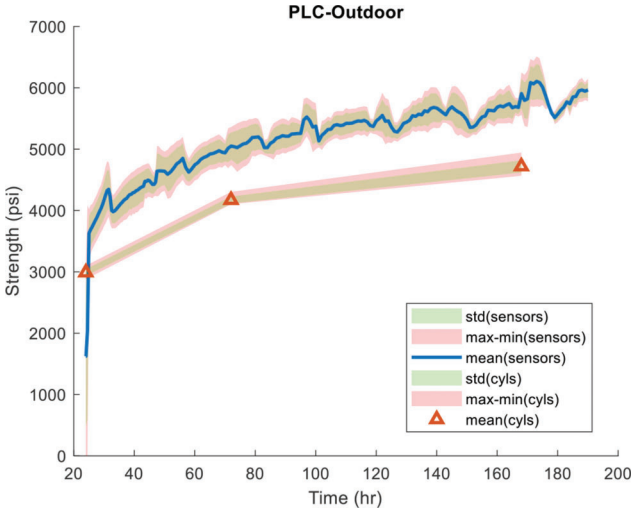

Figure 4.15 Testing results of sensors in PLC concrete cured outdoors.

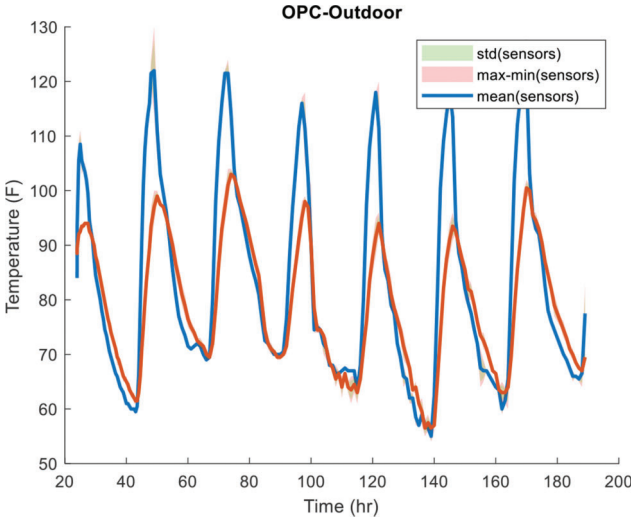

Figure 4.16 Temperature profile of OPC concrete outdoors.

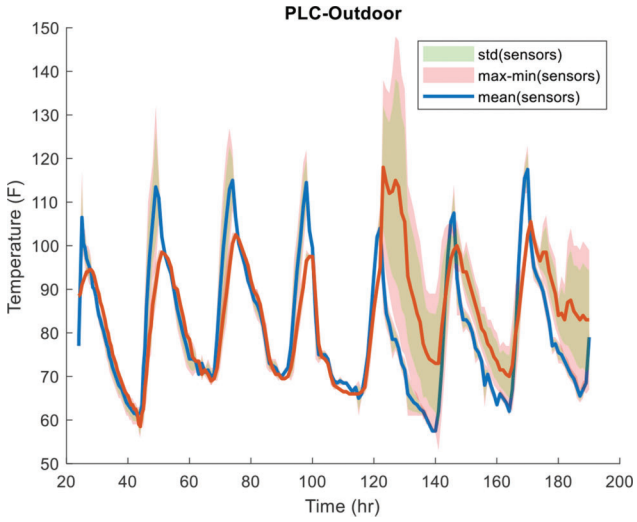

Figure 4.17 Temperature profile of PLC concrete outdoors.

5. FIELD IMPLEMENTATION

This chapter contains the field implementations of the proposed sensor and sensing system (see Table 5.1).

5.1 Center for the Aging Infrastructure (CAI) Testing

A large concrete slab with the dimensions of 12 feet by 8 feet (Figure 5.1) and the thickness of 8 inches was cast in Purdue CAI center at West Lafayette, IN. In addition to the concrete slab, 32 concrete cylinders, with the diameter of 4 inches and length of 8 inches, were cast simultaneously to test the compressive strength development of concrete. The concrete was cast on August 30, 2021, at 8 am.

The testing results are shown in Figure 5.2. The results of two EMI sensors are close to traditional cylinder breaking results at the first 12 hours, and at 24 hours the sensor results tend to overshoot. This is probably due to the error of peak finding for the EMI spectrum. The spectrum got flattened, i.e., the peak almost disappeared, at 24 hours, which could be caused by the structural damage of the sensors. This indicates that the sensors need improvement on its structure design and packaging.

5.2 Bass Road Testing

The sensor and datalogger are deployed in a paving project at Bass Road, Fort Wayne, IN (Figure 5.3). The paving happened on September 2, 2021. The thickness of the pavement is 12 inches. The concrete has water cement ratio of 0.42, and nano-silica (has similar function as fly ash) was incorporated into the concrete. The sensor is fixed on the ground using a steel pin (Figure 5.4). The paver dumped concrete on the ground and consolidate the concrete automatically.

The results are presented in Figure 5.5. It indicates that the sensors survived the paver and the results of two sensors have good consistency. The sensor results are also close to cylinder results.

5.3 Indianapolis Airport Runway Testing

The sensor and datalogger are deployed in a patching project at Indianapolis Airport, Indianapolis, IN

TABLE 5.1
Field Testing Summary Table

Project Type	Infrastructure	Location	Date	Concrete	Thickness
Slab	CAI	West Lafayette, IN	Aug 30, 2021	w/c = 0.45	8 inches
Paving	Bass Rd	Fort Wayne, IN	Sept 02, 2021	w/c = 0.42, nano-silica incorporation	12 inches
Patching	Indy Airport	Indianapolis, IN	Sept 10, 2021	w/c = 0.43, with 40% slag	18 inches
Slab	Shelby Materials	Lapel, IN	July 11, 2022	w/c = 0.42, PLC cement	8 inches
Paving	I-35E Highway	Hillsboro, TX	Aug 29, 2022	w/c = 0.42, PLC cement with 25% fly ash, reinforced	13 inches

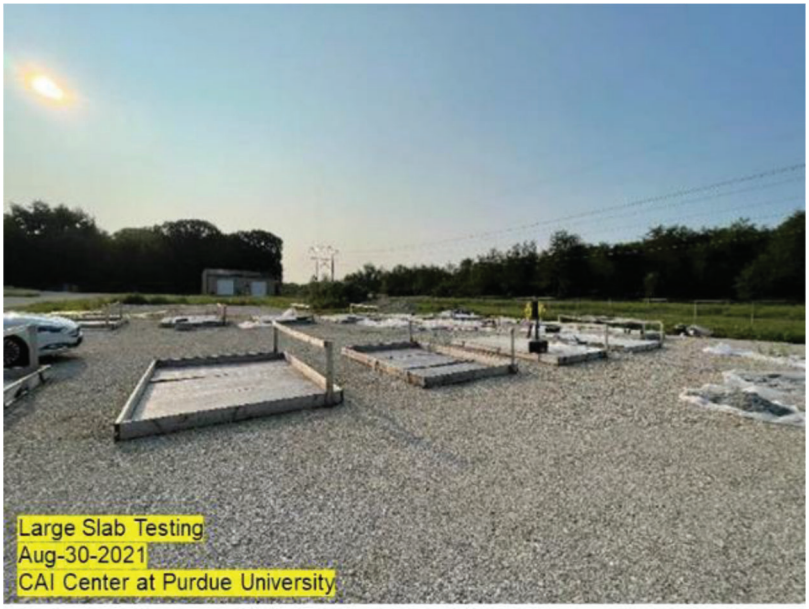

Figure 5.1 CAI field testing photo.

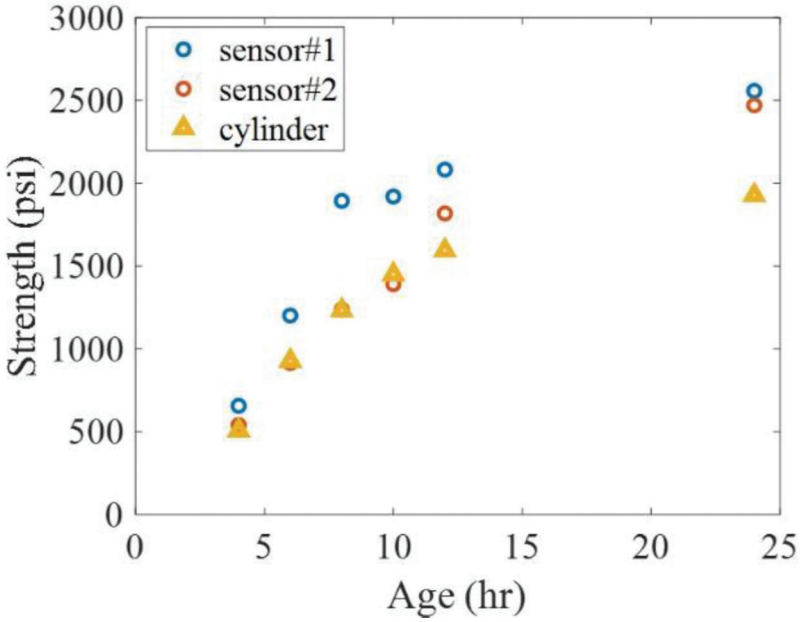

Figure 5.2 CAI field testing results.

Figure 5.3 Bass Road field testing photo.

(Figure 5.6). The concrete of the runway has high portion of slag (40%) for Alkali-Silica Reaction (ASR) prevention. The water cement ratio is 0.43 and the thickness of concrete is 18 inches. This testing was conducted on September 11, 2021. The sensor signals are collected by one of the intermediate versions of the datalogger.

The results shown in Figure 5.7 indicate that the datalogger collected the data continuously from 12 hours to 50 hours after concrete casting. The projection of the strength on 72 hours is close to the cylinder results, whereas the strength result of sensor at 24 hours is about 15% higher than the cylinder result.

5.4 Shelby Materials Ready Mix Plant Testing

The sensor design was evolving in the period January–June 2022. The research team coordinated with a manufacturer at Aurora, IL to produce sensors with standardized workflow. To examine the performance of vendor produced sensors, a large-scale testing was performed at the facility of Shelby Materials at Lapel, IN. Ten concrete beams (6 inches by 6 inches by 22 inches) and one slab (12 feet by 8 feet by 8 inches) were cast on July 11, 2022, as shown in Figure 5.8 and Figure 5.9. Two sensors were placed in each beam and four sensors were placed in the slab. The results are shown in Figure 5.10.

Figure 5.4 Sensor placement on the ground.

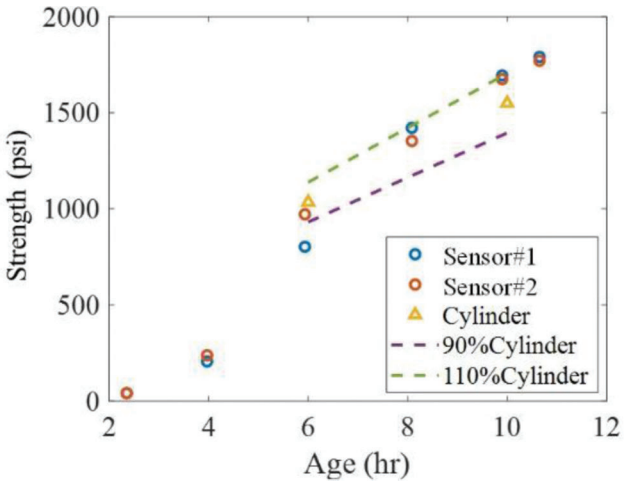

Figure 5.5 Bass Road field testing results.

Figure 5.6 Indianapolis field testing photo.

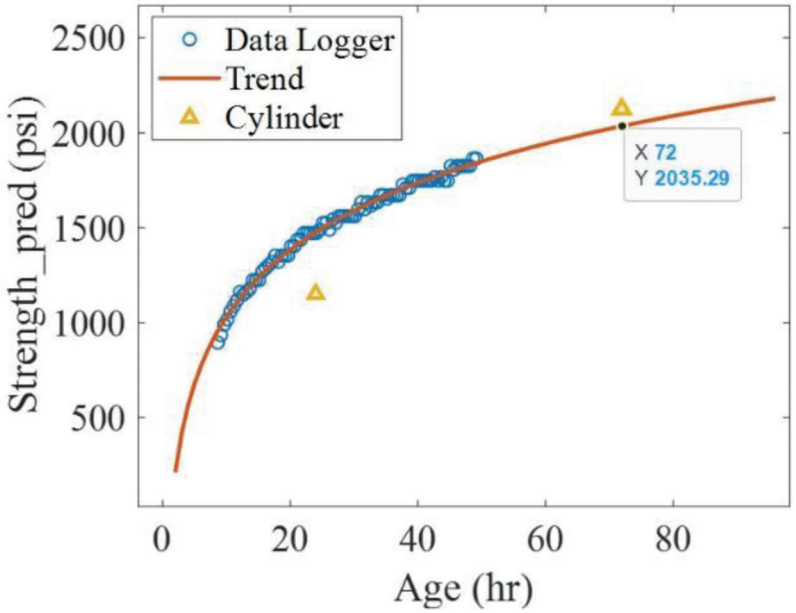

Figure 5.7 Indianapolis field testing results.

Figure 5.8 Sensor placement in beams of Shelby field testing.

Figure 5.9 Concrete casting of the slab of Shelby field testing.

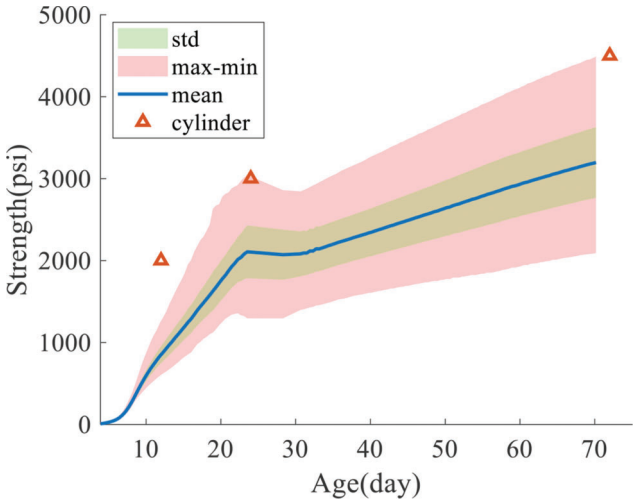

Figure 5.10 Shelby field testing results.

Figure 5.11 I-35E field testing photo.

The mean value, standard deviation, maximum and minimum of sensor results are plotted, along with the cylinder breaking data as the ground truth reference. It is observed that the sensor results are scattered, and the mean value of sensor results are lower than the cylinder breaking results. This may be attributed to the high ambient temperature in July 2022 (around 110°F) and the accelerated hydration temperature for a long period of time (around 120°F for about 10 hours) influenced the sensor reading and caused the separation of sensor between concrete. This hypothesis needs to be further investigated.

5.5 I-35E Interstate Highway Testing

A testing at I-35 highway around Hillsboro, TX was performed to study the performance of sensors in reinforced concrete pavement (Figure 5.11). The concrete has a water cement ratio of 0.42, and 25% fly ash was used to substitute cement. The thickness of the pavement is 13 inch. The reinforcement rebar is located at the middle of the thickness, i.e., 6.5 inches from the ground. Sensors were bounded on rebars using zip ties and plastic tubes. Sensors were embedded at three vertical positions: on the ground, 6.5 inches from the ground and 8 inches from the ground, as shown in Figure 5.12 and Figure 5.13. Testing results are shown in Figure 5.14, Figure 5.15, and Figure 5.16 for three sensor positions, respectively. It can be observed that the sensor at 8 inches from the ground measured higher strength comparing with the sensor on the ground and the sensor at 6.5 inches from the ground. This could be caused by the different hydration speed inside concrete. Another observation is the sensor signal fluctuated and such fluctuation corresponds to daily temperature change, indicating the measurement is sensitive to temperature fluctuations.

Figure 5.12 Sensor placement of I-35E field testing.

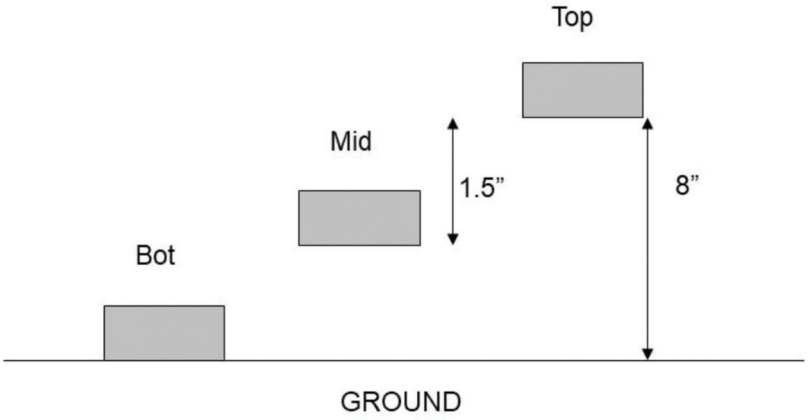

Figure 5.13 Sensor vertical positions of I-35E field testing.

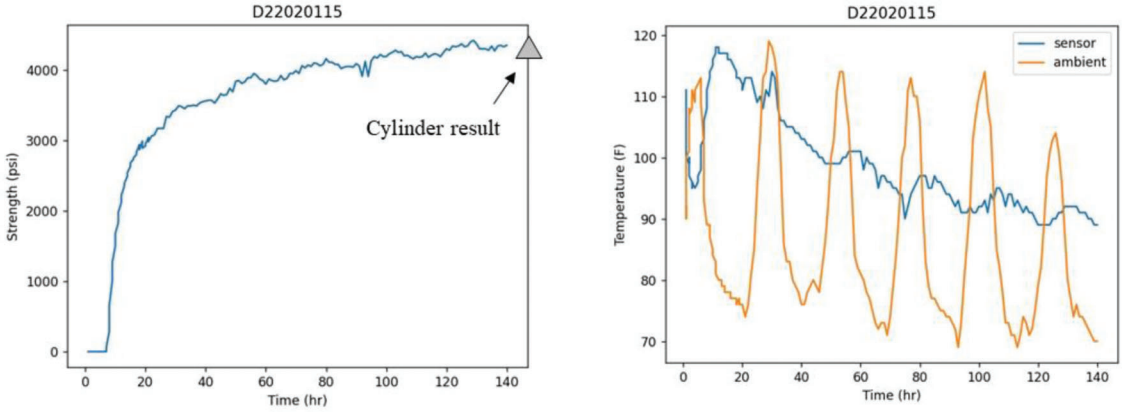

Figure 5.14 I-35E field testing results of the sensor on the ground.

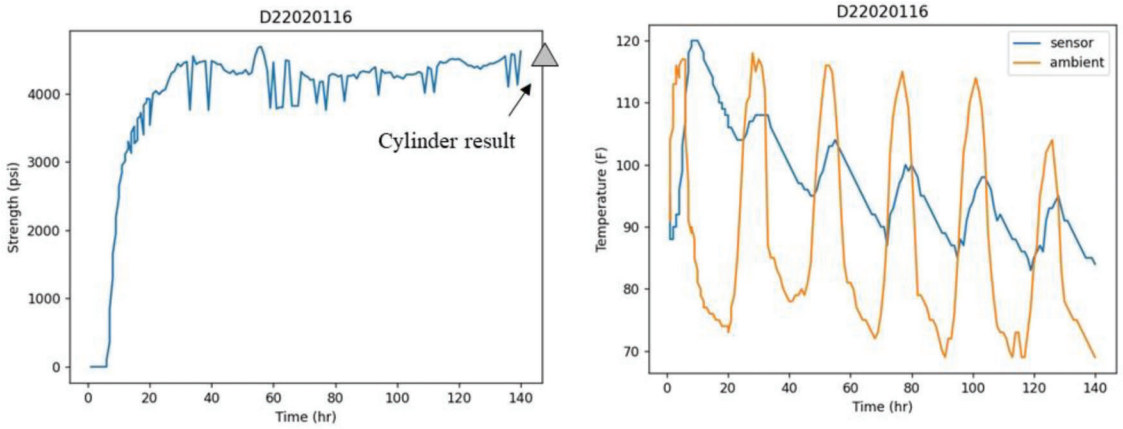

Figure 5.15 I-35E field testing results of the sensor at 6.5 inches above the ground.

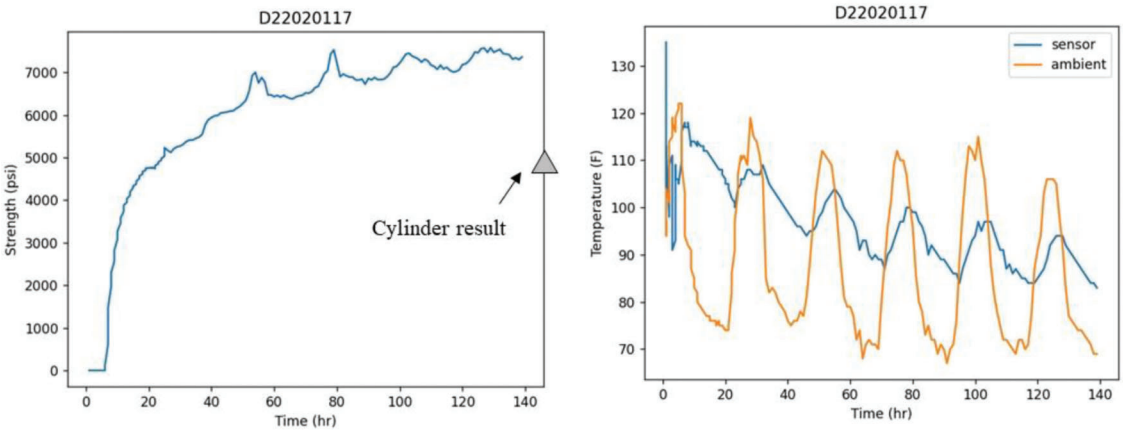

Figure 5.16 I-35E field testing results of the sensor at 8.0 inches above the ground.

6. FINAL CONCLUSIONS AND RECOMMENDATIONS

In this project, the research team developed a manufactured working prototype of cost-effective, on-chip IoT sensing system and approved its feasibility for field testing of concrete strength. The impedance analyzer chip and electrical circuit were explored. The wireless data transmission scheme was tried for Bluetooth and LTE. The sensing mechanism of EMI sensor was renovated and studied through simulation and experiment testing. A series of laboratory and field experiments were performed to learn the capabilities and limitations of the sensing system. The major conclusions of this project are the following.

1. The miniaturized datalogger is developed using customized circuit for data collections and processing. The measured EMI spectrum using the developed datalogger is comparable to commercially available product. The datalogger is powered by rechargeable batteries which can provide power for the sensor for at least 1 month.
2. The datalogger connects to sensors through data cable, whereas the data is transmitted to a remote server through cellular network. The USB cable data pulling function is reserved for applications where there is no cellular network available.
3. A database along with the database management website are developed. The strength is calculated in the website backend based on the EMI spectrum data collected from dataloggers. The website also provides users with the graphic display of data to check real time concrete strength and temperature data.
4. The sensing mechanism of the EMI sensor is renovated. The sensor is packaged using more robust rubber material and stronger resonant peak can be observed in EMI spectrum. The mortar testing shows the variation between resonant frequencies of sensors is about 1.5% COV. The regression function that converts the resonant frequency to concrete strength was developed for laboratory testing and field testing, respectively. The R-square of the regression function for laboratory testing is 0.86, whereas the R-square of the regression function for field testing is 0.64, which may be attributed to the delamination of sensor and concrete under extreme temperature conditions and drastic temperature change.

The recommendations on the practical usage of the outcome of this project are as follows.

1. The datalogger and corresponding database can be used to measure the EMI signal of piezoelectric sensors on site. The datalogger is convenient, affordable, and rugged for concrete projects.
2. The EMI sensor can capture the strength gaining of fresh concrete, the advanced signal processing methods, and conversion from the sensor signal to the absolute concrete strength value are still in progress.
3. The temperature effect, particularly the drastic change of temperature on the sensor packaging and performance needs to be studied further.

REFERENCES

Al-Nu'man, B. S., Aziz, B. R., Abdulla, S. A., & Khaleel, S. E. (2015, August). Compressive strength formula for concrete using ultrasonic pulse velocity. *International Journal of Engineering Trends and Technology*, *26*(1), 9–13.

ASTM. (2019). *Standard test method for fundamental transverse, longitudinal, and torsional resonant frequencies of concrete specimens* (ASTM C215-19). ASTM International. https://doi.org/10.1520/C0215-19

Bhalla, S., & Soh, C. K. (2004a). Structural health monitoring by piezo-impedance transducers. I: Modeling. *Journal of Aerospace Engineering*, *17*(4), 154–165. https://doi.org/10.1061/(ASCE)0893-1321(2004)17:4(154)

Bhalla, S., & Soh, C. K. (2004b). Structural health monitoring by piezo–impedance transducers. II: Applications. *Journal of Aerospace Engineering*, *17*(4), 166–175. https://doi.org/10.1061/(ASCE)0893-1321(2004)17:4(166)

Bogas, J. A., Gomes, M. G., & Gomes, A. (2013, July). Compressive strength evaluation of structural lightweight concrete by non-destructive ultrasonic pulse velocity method. *Ultrasonics*, *53*(5), 962–972. https://doi.org/10.1016/j.ultras.2012.12.012

Carino, N. J., Sansalone, M., & Hsu, N. N. (1986, March). A point source-point receiver, pulse-echo technique for flaw detection in concrete. *Journal of the American Concrete Institute*, *83*(2), 199–208.

Carpenter, T. M., Cowell, D. M. J., & Freear, S. (2018, October). Real-time FIR filter equalisation of analog front ends for soft-tissue quantitative ultrasound. In *2018 IEEE international ultrasonics symposium (IUS)*. Kobe, Japan. https://doi.org/10.1109/ULTSYM.2018.8579691

Cheng, C.-C., & Sansalone, M. (1993). The impact-echo response of concrete plates containing delaminations: Numerical, experimental and field studies. *Materials and Structures*, *26*(5), 274–285.

del Viso, J. R., Carmona, J. R., & Ruiz, G. (2008, March). Shape and size effects on the compressive strength of high-strength concrete. *Cement and Concrete Research*, *38*(3), 386–395. https://doi.org/10.1016/j.cemconres.2007.09.020

Diaferio, M., & Vitti, M. (2021). Correlation curves to characterize concrete strength by means of UPV tests. *Proceedings of 1st International Conference on Structural Damage Modelling and Assessment* (pp. 209–218).

Fan, S., Zhao, S., Qi, B., & Kong, Q. (2018, May). Damage evaluation of concrete column under impact load using a piezoelectric-based EMI technique. *Sensors*, *18*(5), 1591. https://doi.org/10.3390/s18051591

Feng, Q., Liang, Y., & Song, G. (2019, January). Real-time monitoring of early-age concrete strength using piezoceramic-based smart aggregates. *Journal of Aerospace Engineering*, *32*(1), 04018115. https://doi.org/10.1061/(ASCE)AS.1943-5525.0000939

FHWA. (2005, November). *Maturity testing for concrete pavement applications tech brief* (Report No. FHWA-IF-06-004). Federal Highway Administration.

Gibson, A., & Popovics, J. S. (2005, April). Lamb wave basis for impact-echo method analysis. *Journal of Engineering Mechanics*, *131*(4), 438–443. https://doi.org/10.1061/(ASCE)0733-9399(2005)131:4(438)

Hou, S., Kong, Z., He, J., & Wu, B. (2019, July). Geometry-independent attenuation and randomness of ultrasound wave propagation in concrete measured by embedded PZT transducers. *Smart Material Structure*, *28*(7), 075004. https://doi.org/10.1088/1361-665X/ab1ced

Ju, M., Park, K., & Oh, H. (2017, December). Estimation of compressive strength of high strength concrete using non-destructive technique and concrete core strength. *Applied Sciences*, *7*(12), 1249. https://doi.org/10.3390/app7121249

Kewalramani, M. A., & Gupta, R. (2006, May). Concrete compressive strength prediction using ultrasonic pulse velocity through artificial neural networks. *Automation in Construction*, *15*(3), 374–379.

Kolluru, S., Popovics, J., & Shah, S. (2000). Determining elastic properties of concrete using vibrational resonance frequencies of standard test cylinders. *Cement, Concrete, and Aggregates*, *22*(2), 81–89. https://doi.org/10.1520/CCA10467J

Kong, Q., Hou, S., Ji, Q., Mo, Y. L., & Song, G. (2013, August). Very early age concrete hydration characterization monitoring using piezoceramic based smart aggregates. *Smart Material Structure*, *22*(8), 085025. https://doi.org/10.1088/0964-1726/22/8/085025

Lee, B. J., Kee, S.-H., Oh, T., & Kim, Y.-Y. (2017). Evaluating the dynamic elastic modulus of concrete using shear-wave velocity measurements. *Advances in Materials Science and Engineering*, 2017, 1–13. https://doi.org/10.1155/2017/1651753

Liang, C., Sun, F. P., & Rogers, C. A. (1994, January). An impedance method for dynamic analysis of active material systems. *Journal of Vibration and Acoustics*, *116*(1), 120–128. https://doi.org/10.1115/1.2930387

Lu, X., Lim, Y. Y., & Soh, C. K. (2018, July). A novel electromechanical impedance–based model for strength development monitoring of cementitious materials. *Structural Health Monitoring*, *17*(4), 902–918. https://doi.org/10.1177/1475921717725028

Luo, Z., Deng, H., Li, L., & Luo, M. (2020, November). A simple PZT transducer design for electromechanical impedance (EMI)-based multi-sensing interrogation. *Journal of Civil Structural Health Monitoring*, *11*, 235–249. https://doi.org/10.1007/s13349-020-00449-6

Mahure, N. V., Vijh, G. K., Sharma, P., Sivakumar, N., & Ratnam, M. (2011, October). Correlation between pulse velocity and compressive strength of concrete. *International Journal of Earth Sciences and Engineering*, *4*(6), 871–874.

Narayanan, A., Kocherla, A., & Subramaniam, K. V. L. (2017, December). Embedded PZT sensor for monitoring mechanical impedance of hydrating cementitious materials. *Journal Nondestructive Evaluation*, *36*(64). https://doi.org/10.1007/s10921-017-0442-4

Providakis, C., & Liarakos, E. (2011). T-WiEYE: An early-age concrete strength development monitoring and miniaturized wireless impedance sensing system. *Procedia Engineering*, *10*, 484–489.

Ryden, N. (2011, January). Resonant frequency testing of cylindrical asphalt samples. *European Journal of Environmental and Civil Engineering*, *15*(4), 587–600. https://doi.org/10.1080/19648189.2011.9693349

Sadri, A. (2003). Application of impact-echo technique in diagnoses and repair of stone masonry structures. *NDT & E International*, *36*(4), 195–202.

Sansalone, M. (1997). Impact-echo: The complete story. *Structural Journal*, *94*(6), 777–786.

Saravanan, T., Kalyanasundaram, B., Priya, C. B., Reddy, A. L., & Gopalakrishnan, N. (2015). Comparative performance of various smart aggregates during strength gain and damage states of concrete. *Smart Materials and Structures*, *24*(8), 085016.

Shariati, M., Ramli-Sulong, H., Arabnejad, K. H. M., Shafigh, P., & Sinaei, H. (2011). Assessing the strength of reinforced concrete structures through ultrasonic pulse velocity and Schmidt rebound hammer tests. *Science Research and Essays*, *6*(1), 213–220.

Shin, S. W., Qureshi, A. R., Lee, J.-Y., & Yun, C. B. (2008, October). Piezoelectric sensor based nondestructive active monitoring of strength gain in concrete. *Smart Material Structure*, *17*(5), 055002. https://doi.org/10.1088/0964-1726/17/5/055002

Su, Y.-F., Han, G., Amran, A., Nantung, T., & Lu, N. (2019, November). Instantaneous monitoring the early age properties of cementitious materials using PZT-based electromechanical impedance (EMI) technique. *Construction and Building Materials*, *225*, 340–347. https://doi.org/10.1016/j.conbuildmat.2019.07.164

Trtnik, G., Kavčič, F., & Turk, G. (2009). Prediction of concrete strength using ultrasonic pulse velocity and artificial neural networks. *Ultrasonics*, *49*(1), 53–60.

Wang, D., Song, H., & Zhu, H. (2014, October). Embedded 3D electromechanical impedance model for strength monitoring of concrete using a PZT transducer. *Smart Material Structure*, *23*(11), 115019. https://doi.org/10.1088/0964-1726/23/11/115019

Wang, T., Wei, D., Shao, J., Li, Y., & Song, G. (2018, November). Structural stress monitoring based on piezoelectric impedance frequency shift. *Journal of Aerospace Engineering*, *31*(6), 04018092. https://doi.org/10.1061/(ASCE)AS.1943-5525.0000900

Yang, Y., & Divsholi, B. S. (2010, December). Sub-frequency interval approach in electromechanical impedance technique for concrete structure health monitoring. *Sensors*, *10*(12), 11644–11661. https://doi.org/10.3390/s101211644

Zhang, H., Hou, S., & Ou, J. (2019, July). SA-based concrete seismic stress monitoring: The influence of non-uniform stress fields. *Engineering Structures*, *190*, 66–75. https://doi.org/10.1016/j.engstruct.2019.03.113

About the Joint Transportation Research Program (JTRP)

On March 11, 1937, the Indiana Legislature passed an act which authorized the Indiana State Highway Commission to cooperate with and assist Purdue University in developing the best methods of improving and maintaining the highways of the state and the respective counties thereof. That collaborative effort was called the Joint Highway Research Project (JHRP). In 1997 the collaborative venture was renamed as the Joint Transportation Research Program (JTRP) to reflect the state and national efforts to integrate the management and operation of various transportation modes.

The first studies of JHRP were concerned with Test Road No. 1—evaluation of the weathering characteristics of stabilized materials. After World War II, the JHRP program grew substantially and was regularly producing technical reports. Over 1,600 technical reports are now available, published as part of the JHRP and subsequently JTRP collaborative venture between Purdue University and what is now the Indiana Department of Transportation.

Free online access to all reports is provided through a unique collaboration between JTRP and Purdue Libraries. These are available at http://docs.lib.purdue.edu/jtrp.

Further information about JTRP and its current research program is available at http://www.purdue.edu/jtrp.

About This Report

An open access version of this publication is available online. See the URL in the citation below.

Kong, Z., & Lu, N. (2023). *Determining optimal traffic opening time through concrete strength monitoring: Wireless sensing* (Joint Transportation Research Program Publication No. FHWA/IN/JTRP-2023/05). West Lafayette, IN: Purdue University. https://doi.org/10.5703/1288284317613